Dear editor,

we addressed all points raised by the referees and responded positive to most of them.

Major modifications:

a) Clarification of ON yields and $OrgNO_3$ fractions throughout the manuscript. We provided a new Figure 4 to better address these issues. We modified the discussion of ON and $OrgNO_3$ in section 4.1 and 4.3.
b) We addressed the role of alkoxy radicals in the modified Figure 3 and showed that their fragmentation is probably not important for the SOA yields. We reformulated section 4.4. and the conclusion section 5, accordingly.
c) For new Figure 3 and new Figure 4 we replaced simple integration of UMR data by analysis based on assigned high resolution CIMS data. The mass ranges 230-550 Da were kept the same. As a consequence the values are somewhat lower now, but that affected none of our conclusions. We now strictly refer to mass concentrations in Figures 3, 4, and 9. For consistency we also made a new Figure 9, now also based on HR data.
d) Wherever requested we modified the text of the manuscript for better reading and understanding, e.g. sections 2.4, 3.3, 3.5, 4.1, 4.4 and 5.
e) We tried to explain uptake experiments and Zhao et al. experiments more clearly.
f) We updated the references for the discussions of ON and $OrgNO_3$ hydrolysis, as well as for particulate ON and SOA yields as $f(NO_X)$.
g) We went through the manuscript and tried to remove grammatical errors.

With best regards !

Thomas Mentel

Reply to reviewer #1

We thank the reviewer #1 for the helpful comments. We addressed all points raised.

Reviewer comment:

1. The paper concluded with increasing NOX HOM-ACC strongly decreases and consequently suppress SOA formation. While the experiments and analysis appear robust and in agreement with some literature, it is important to point out that some other literature such as Pye et al., (2015) and Marais et al. (2016), with specific representation of particulate organic nitrate predict the reduction in NOx emissions causes a considerable reduction in organic aerosol. Could authors comment on this discrepancy? In this regard, in Figure 2 authors showed HOM spectra with and without NOX addition. It might be worthwhile to mention total SOA or HOM mass for these two cases for easier comparison.

Reply:
In our paper Safrazadeh et al. (2016) we showed that the effect of NO_X on SOA yields is complex. NO_X can affect SOA formation by influencing the OH concentration (a variation of OH scavenging as described in McFiggans et al. (2019)) and by changing the product composition. How the product composition and the product properties are changing with NO_X has general components, such as NO reacting fast with RO_2, and is specific for the compound (class) under consideration.
Marais et al. (2016) propose an improved mechanism for isoprene oxidation and applied it in a regional model study. They showed that increasing NO_X (NO) is leading to decreasing *isoprene* SOA: “Isoprene SOA concentrations increase as NOx emissions decrease (favoring the low-NOx pathway for isoprene oxidation).” Herein the low-NO_X pathway leads to the formation of IEPOX, which in turn enter the particulate phase by reactive uptake. The reactive uptake of IEPOX is specific to isoprene reaction systems, and we don’t really see what could be learned from that comparison for our study of monoterpenes.
The work of Pye et al. (2015) is also a regional model study considering the role of NO and NO_3 in organic nitrate (ON) formation. The results of regional model studies depend on parametrization of the precursor chemistry (which is in this case lumped), while we describe specific observations in our chamber. Pye et al. find a decrease of 9% in SOA when NO_X emissions are reduced by 25%. The NO_X level was roughly of the order of one 1 ppb, the effect of the NO_X reduction on the NO_X concentration was not specified. Pye et al. attributed the monoterpene-SOA decrease with decreasing NO_X mainly to a decreasing NO_3 contribution. Effects of NO_3 are outside our observations, and we added a statement in the Introduction section, underling that our study focus on NO_X in daytime photochemical systems and that NO_3 reactions also lead to ON, but are not treated here (p.2, line 16-20, in the revised manuscript).
Since Marais et al. as well as Pye et al. address aspects different than our study, it is very difficult to say if their model results are in contradiction to ours or not. So, detailed specific comparisons with Marais et al. or Pye et al. do not make much sense to us. However, the referee is correct that our laboratory results, which address mechanistic aspects of SOA formation in the presence of NO_X especially under consideration of HON-ON, should not be generalized too quickly and blindly transferred to the atmosphere, where more aerosol precursors and SOA formation processes prevail. In order to prevent misleading interpretations of our specific results we will add a sentence in the concluding section (p.23, line 26-31, in the revised manuscript):

“Note, that we considered the photochemistry of NO_X to SOA contribution for two major MT, α-pinene and β-pinene. We find that that SOA yields are fairly independent of NO_X, but drop significantly at the highest NO_X levels. Model studies show that increase of NO_X emissions may also lead to more SOA, when NO_3 is the oxidant (e.g. Pye et al. 2015) or when isoprene is involved (Marais et al. 2016). In the latter case NO directs the gas phase mechanism toward isoprene products with reactive uptake, while for compounds like α-pinene and β-pinene, which were investigated here, condensation is more important for SOA formation and thus vapor pressures controls SOA yields.”

We did not modify Figure 2 as this illustrates how the effect of NO_X appears quite obvious in the mass spectra. Instead we modified Figure 3, which now shows mass concentrations of total HOM and of monomers and accretion products. These were derived from high resolution analysis of the mass spectra, as this allowed for a more detailed analysis. We replaced integration of mass spectra at UMR in certain ranges by analysis based on peak lists (Suppl. S6). We can thus resolve monomers and accretion products in the overlapping range. Identified peaks explain more than 90% of the observed signal. We also replaced mixing ratio by mass concentration as this allows for a better direct estimate how much mass monomers and accretion products potentially contribute to SOA. We limited the analysis to the mass range 230-550Da, which covers the compounds with sufficient functionalization to condense and form SOA. Therefore the numbers are somewhat lower compared to the original manuscript, but this did not affect any of the conclusions.
With new Figure 3 we also modified formulations in section 3.3 (p.12, line 26 – p.13, line12, in the revised manuscript).

2. Page 11, Line 2
a) The authors estimated a molar yield of ≈36% for the ON formed from β–pinene which is higher than the largest previously reported values (26 ±7% Rindelaub et al., (2016), while for similar condition of this study (acidic seed aerosol and RH ≈60%), they even estimated less (≈6%).
b) The authors mentioned at the Figure 9’s caption “The effect of hydrolysis of 80% of the organic bound nitrate has no substantial effect on the SOA mass.” However, Boyd et al. (2015) estimated particle phase hydrolysis of organic nitrates compose 45–74% of the organic aerosol. These discrepancies might be attributed to estimation of a slower aerosol hydrolysis in this study? and subsequently underestimation of importance of hydrolysis for explaining the SOA mass suppression with increasing NOX in the system?

Reply:
a) Our molar yield considers the sum of all organic nitrates formed from β-pinene in the gas-phase in absence of seed aerosol at RH = 60%. Our finding is commensurable with molar branching ratios of the reaction RO_2 + NO into RO and ON as implemented in MCMv3.1.1 for ß-pinene for the given conditions. Since we did not have seed aerosols in this experiment, the observed molar yield cannot be dependent on the pH of the seed aerosols. ON formation depends of course both on the VOC under investigation and on the VOC/NOX ratio. Therefore one cannot expect the same yields in different studies with different precursor starting conditions.

Rindlaub et al. (2015) investigated α-pinene and reported an apparent yield for ON of 26(±7)% by extrapolation to particle free conditions. Assuming that α-pinene and β-pinene have a similar ON/RO branching ratio in the reaction of RO_2 with NO/NO_2 this value is within the errors the same as our 36(±4)%. While Rindelaub et al. observed the integral ON by actively measuring the available ON by FTIR, we derive our value from the consumption of NO_2, more precisely from the excess of NO_2 in the absence of β-pinene at the same OH concentration. So, as long as the branching ON/RO does not much depend on RH, which is the case, we would observe by our method the same apparent ON yield at all RH, while Rindelaub et al. would miss the hydrolysed ON. It is not on us to judge Rindelaub's et al. work, but it was performed for another compound, α-pinene, at ppm initial concentrations and more than 100ppb of NO_X initially in the system. Moreover, there were several hundred to several thousand ug/m^3 particulate mass formed during their non-seeded experiments, so a substantial fraction of the ON, including semivolatile ON, must have resided in the particulate phase. In our interpretation of their Figure 4 they observed overall a yield of ON of 5-10% for a wide range of RH with strong excursions up to 23% in a narrow range around 15% RH.
We reformulated a part of section 3.5 to include references proposed by the reviewer (p.17, line 8-13, in the revised manuscript).

b) The intent of our study is clearly *not* to solve the question of hydrolysis of particulate ON. Our starting point of discussing HOM-ON hydrolysis is to find a rationale for the mismatch between observed $OrgNO_3$ (particulate organic bound nitrate) observed by AMS (up to 3%) and the $OrgNO_3$ which should be expected from the uptake/condensation of HOM, including HOM-ON, with more than 6 O (up to 10%). The mismatch indicated that more than 2/3 of the $OrgNO_3$ got somehow lost. Nevertheless, as shown in Figure 9, the role of hydrolysis for the impact of NO_X for SOA production is negligible. Since this has been proposed in the literature, we were merely wondering if hydrolysis of ON in the particulate phase may help to reconcile particulate phase observations and HOM-ON.
Our Figure 6 shows that vapor pressures of HOM do not depend much on the type of the termination group. It seems realistic to us that only HNO_3 will escape the particulate phase on hydrolysis of multi-functionalized HOM-ON, while the multi-functionalized organic moieties remain. Under this specific case/assumption we calculated the change of the expected mass as shown in Figure 9; it assumes in fact instantaneous, thus fast hydrolysis. The release of HNO_3 can explain the mismatch between gas phase $OrgNO_3$ that is expected to condense on particles and realized $OrgNO_3$ in the particulate phase. Figure 9 is supposed to show that this type of hydrolysis will not much affect the SOA mass thus our finding of a low dependence of SOA yield on NO_X, if *OH concentration is kept stable*. The somewhat lower yields at high NO_X in our case can be solely accounted for by less mass formation due to HOM by suppression of dimers with increasing NO_X. Overall, our interpretation is not in contradiction with field and model studies which detected that about 2/3 of the particulate ON hydrolyze and release HNO_3 from the particulate phase (Zare et al., 2019, Fisher et al., 2016). Like Takeuchi and Ng (2019), these studies leave the fate of the organic moieties open, but they are likely alcohols (Hu et al. 2011) and thus have the same or lower vapor pressures as the mother ON (Zare et al., 2019).
We are aware of and appreciate the study by Boyd et al. 2015. However here must be a misunderstanding. First of all, Boyd et al. investigated the oxidation of β-pinene by NO_3. Herein NO_3 is the primary oxidant forming nitrate groups directly by first attack on the double bond. This is different from our study where we oxidize the MT by OH and (HOM-)ON are formed by peroxy radicals terminating with NO and NO_2. Boyd et al. found 45-74% contribution of particulate ON of which 90% survived hydrolysis, due to a lower fraction of tertiary ON in NO_3 oxidation compared to photooxidation and termination by NO_X (our case).

Browne et al. (2013) suggested that photooxidation of α-pinene and termination by NO_X produces about 60% tertiary ON that easily hydrolyze, but they considered ON hydrolysis only for HNO_3 budget. The suggestion by Browne et al. would be perfectly in line with our interpretation, that about 2/3 of the $OrgNO_3$ is lost as HNO_3. Takeuchi and Ng (2019) stated in a recent paper that they cannot determine for sure the "fate of the organic moiety of the hydrolysis product (i.e., stay in the particle phase or repartition back to the gas phase)". The hydrolysis was observed by Takeuchi and Ng for about the same relative humidity. The hydrolyzable fraction FH for α-pinene +OH + NO system was 32%, if one assumes no loss of the organic moiety. A hydrolyzed fraction of 32% is about half what we determined, but regarding our only rough estimates it is within the errors. The hydrolysis was fast and we are able to easily observe it within the residence time of 1h in our chamber. Taken all together the findings of the Boyd et al, Browne et al. (2013), and Takeuchi and Ng l. are supportive or at least not in contradiction to our findings. Furthermore, the experiment of Zhao et al. (2018) showed that expected $OrgNO_3$ and observed $OrgNO_3$ agree in a dry environment. These experiments were made in another context but with the same instruments and analysis methods. Together with most of the literature data this all is in favor of our interpretations. However, we would like to note that hydrolysis of ON and pON is not the focus of the paper and our data are not suited to solve inconclusive findings in the literature.

3) Page 18, Line 11-24 The authors discussed higher humidity in their chamber and hydrolysis as the key for less estimation of $OrgNO_3$ fraction in the particulate-phase than as determined by AMS and also finding (≈11%) by Zhao et al. (2018). It is important to point out not only Zhao et al. but also many recent measurements (e.g., Romer et al., 2016) and modeling studies (e.g., Pye et al., 2015; Fisher et al., 2016; Zare et al., 2019) estimated a higher fraction of organic nitrates in the particle phase (≈10%-20%). As they also considered a rather fast hydrolysis for organic nitrate aerosols it might be worthwhile to compare the result here to their results as well. However, it might be useful to mention Zare et al. show that at a more humid condition (similar to this study with higher RH) heterogeneous uptake to particle water tends to form less particulate organic nitrates against uptake to dry organic aerosols. Considering the impact of humidity at the aerosol formation together with the impact on the loss process of hydrolysis for particulate organic nitrates could help reconcile the discrepancy?

Reply:
We think here is a misunderstanding. As was shown in Figure 8 (blue and orange circles) the molar fraction of particulate ON expected from HOM condensation ranges up to 40% for both MT with increasing NO_X. In the new Figure 4 we show now that the mass fraction of HOM-ON mounted up to 50%. From this point of view we are cum granis sale in agreement with the other lab, field and model studies which find similar fractions of particulate ON from MT. The diagnostic link between HOM-ON and particulate phase analysis by AMS was organic bound nitrate ($OrgNO_3$), a terminus used by the AMS community. We discuss $OrgNO_3$, i.e. the mass fraction of $–NO_3$ groups attached to ON. In Figure 8 we showed the $OrgNO_3$ mass fraction expected from condensable HOM-ON and compare it with the $OrgNO_3$ fraction observed by AMS. We tried to clarify the difference between $OrgNO_3$ and particulate ON throughout the manuscript, e.g. we added a note to section 2.3 (p.8, line 16-17, in the revised

manuscript), reformulated large parts of section 4.1. (p.18, line 2-15, in the revised manuscript) and (p.18, line 22-23, in the revised manuscript).
We attributed the discrepancy between $OrgNO_3$ in the gas-phase HOM and in the particle phase to plausible hydrolysis of ON in the particulate phase (as discussed in the previous reply). Since we are missing organic bound NO_3 in the system and *not* SOA mass, we assumed that only HNO_3 is released to the gas-phase. As shown in Figure 9 this effect is small, because $OrgNO_3$ contributed only about 20% to HOM-ON mass and HOM-ON contributes a few times 10% percent to SOA mass.
The HOM-ON hydrolysis in the particulate phase must occur on times scales of less than one hour at 60%RH. The time scale is in accordance with the findings of Romer et al. (2016), however they linked ON hydrolysis to isoprene oxidation, which we don't have. We choose Zhao et al. as an example for expected $OrgNO_3$ and observed $OrgNO_3$ being in agreement in a dry environment, because they used the same instruments and analysis methods.
We determined effective uptake rates for HOM-ON and the $OrgNO_3$ content in the particulate phase at only one relative humidity. We did not determine effective uptake rates for HOM ON at different humidity and therefore our data do not allow statements on the effects of humidity on particle formation by condensation of HOM.
Although hydrolysis of ON is very interesting and the most plausible explanation for the loss of $OrgNO_3$, it is not a central point of out studies and we prefer to refrain from further discussion in the manuscript.

We modified Figure 4 substantially in order to show the mass fraction of HOM-ON.

We added the references (see below) for discussion here to manuscript.

Minor comments
We are sorry for that many mistakes and typos. We thank the reviewer for the careful reading of the manuscript and for the corrections. We went through the manuscript in order to improve language and grammar.

Page 3, for less confusion and similar to the other relevant papers, it is better to give a same reaction number for reactions with similar reactants, e.g. (R4) and (R4a) should be "(R4a)" and "(R4b)", and also for R5 and R7 should change as "(R5a)" and "(R5b)".
done

Page 6, Line 1-4, multiplication sign for reaction rates are missed.
dots replaced by x

Page 6, Line 2, References should be lined up in the proper sequence.
done

Page 13, Line 13, remove spare space before parentheses.
done

Page 15, Line 1-4, remove redundant parentheses.
We could not find redundant parenthesis. The parenthesis being there were set by purpose to indicate a side remark.
No action.

Page 15, Line 21, remove extra “was”
done

Page 15, line 24, “estimated to be”
done

Page 32, Figure1, for better readability write axis label on the right-hand side from
done, for consistency also applied to Figure 7

Page 37, Line4, the brown bars look like more “orangeish” than brown in my eyes.
color tuned to brown

Page 40, Line 5-6 used different font.
corrected

References

Boyd, C. M., Sanchez, J., Xu, L., Eugene, A. J., Nah, T., Tuet, W. Y., Guzman, M. I., and Ng, N. L.: Secondary organic aerosol formation from the β-pinene+NO_3 system: effect of humidity and peroxy radical fate, Atmos. Chem. Phys., 15, 7497-7522, 10.5194/acp-15-7497-2015, 2015.

Browne, E. C., Min, K. E., Wooldridge, P. J., Apel, E., Blake, D. R., Brune, W. H., Cantrell, C. A., Cubison, M. J., Diskin, G. S., Jimenez, J. L., Weinheimer, A. J., Wennberg, P. O., Wisthaler, A., and Cohen, R. C.: Observations of total RONO2 over the boreal forest: NOx sinks and HNO_3 sources, Atmos. Chem. Phys., 13, 4543-4562, 10.5194/acp-13-4543-2013, 2013.

Fisher, J. A., Jacob, D. J., Travis, K. R., Kim, P. S., Marais, E. A., Chan Miller, C., Yu, K., Zhu, L., Yantosca, R. M., Sulprizio, M. P., Mao, J., Wennberg, P. O., Crounse, J. D., Teng, A. P., Nguyen, T. B., St. Clair, J. M., Cohen, R. C., Romer, P., Nault, B. A., Wooldridge, P. J., Jimenez, J. L., Campuzano-Jost, P., Day, D. A., Hu, W., Shepson, P. B., Xiong, F., Blake, D. R., Goldstein, A. H., Misztal, P. K., Hanisco, T. F., Wolfe, G. M., Ryerson, T. B., Wisthaler, A., and Mikoviny, T.: Organic nitrate chemistry and its implications for nitrogen budgets in an isoprene- and monoterpene-rich atmosphere: constraints from aircraft (SEAC4RS) and ground-based (SOAS) observations in the Southeast US, Atmos. Chem. Phys., 16, 5969-5991, 10.5194/acp-16-5969-2016, 2016.

Hu, K. S., Darer, A. I., and Elrod, M. J.: Thermodynamics and kinetics of the hydrolysis of atmospherically relevant organonitrates and organosulfates, Atmos. Chem. and Phys., 11, 8307-8320, 10.5194/acp-11-8307-2011, 2011.

Marais, E. A., Jacob, D. J., Jimenez, J. L., Campuzano-Jost, P., Day, D. A., Hu, W., Krechmer, J., Zhu, L., Kim, P. S., Miller, C. C., Fisher, J. A., Travis, K., Yu, K., Hanisco, T. F., Wolfe, G. M., Arkinson, H. L., Pye, H. O. T., Froyd, K. D., Liao, J., and McNeill, V. F.: Aqueous-phase mechanism for secondary organic aerosol formation from isoprene: application to the southeast United States and co-benefit of SO2 emission controls, Atmos. Chem. Phys., 16, 1603-1618, 10.5194/acp-16-1603-2016, 2016.

Pye, H. O. T., Luecken, D. J., Xu, L., Boyd, C. M., Ng, N. L., Baker, K. R., Ayres, B. R., Bash, J. O., Baumann, K., Carter, W. P. L., Edgerton, E., Fry, J. L., Hutzell, W. T., Schwede,

D. B., and Shepson, P. B.: Modeling the Current and Future Roles of Particulate Organic Nitrates in the Southeastern United States, Environmental Science & Technology, 49, 14195-14203, 10.1021/acs.est.5b03738, 2015.

Rindelaub, J. D., McAvey, K. M., and Shepson, P. B.: The photochemical production of organic nitrates from alpha-pinene and loss via acid-dependent particle phase hydrolysis, Atmos. Environ., 100, 193-201, 10.1016/j.atmosenv.2014.11.010, 2015.

Romer, P. S., Duffey, K. C., Wooldridge, P. J., Allen, H. M., Ayres, B. R., Brown, S. S., Brune, W. H., Crounse, J. D., de Gouw, J., Draper, D. C., Feiner, P. A., Fry, J. L., Goldstein, A. H., Koss, A., Misztal, P. K., Nguyen, T. B., Olson, K., Teng, A. P., Wennberg, P. O., Wild, R. J., Zhang, L., and Cohen, R. C.: The lifetime of nitrogen oxides in an isoprene-dominated forest, Atmos. Chem. Phys., 16, 7623-7637, 10.5194/acp-16-7623-2016, 2016.

Takeuchi, M., and Ng, N. L.: Chemical composition and hydrolysis of organic nitrate aerosol formed from hydroxyl and nitrate radical oxidation of α-pinene and β-pinene, Atmos. Chem. Phys., 19, 12749-12766, 10.5194/acp-19-12749-2019, 2019.

Zare, A., Fahey, K. M., Sarwar, G., Cohen, R. C., and Pye, H. O. T.: Vapor-Pressure Pathways Initiate but Hydrolysis Products Dominate the Aerosol Estimated from Organic Nitrates, ACSEarthSpaceChem., 3, 1426-1437, 10.1021/acsearthspacechem.9b00067, 2019.

Reply to reviewer #2

We thank the reviewer #2 for the helpful comments. We addressed all points raised.

Comments of Referee #2

The goal of this work is to explore the observed and documented suppression of SOA formation in the presence of NOx from previous studies. The authors hypothesized the observed decrease in SOA mass could be due to HOM termination reactions, in particular the reactions that form gas-phase accretion products or HOM organic nitrates. To test their hypothesis, they performed a series of chamber experiments at the Jülich Plant Atmosphere Chamber, a well characterized environment. They primarily used a Chemical Ionization Mass Spectrometer with NO3- ionization which has been repeatedly shown to be useful in measuring HOM, and studied the photooxidation of _and _-pinene. They found that HOM accretion products were much more heavily suppressed than non-nitrate monomer products in the presence of NOx. They determine this loss of accretion products is a possible and even likely reason for SOA mass suppression in the presence of NOx.

Section 4.4 discusses the suppression of accretion products but notably lacking is the possibility of precursor decomposition as a result of RO2 + NO (R7, page 3 line 24) forming an alkoxy which can rapidly decompose, resulting in smaller RO2 building blocks for accretion chemistry. This is brought up briefly on page 11 line 23, but is not worked into the discussion in section 4.4. It is however noted in the last sentence of the manuscript, only to say that it will be discussed in a further manuscript. This seems warranted to be discussed within this manuscript, and as-is I find it to be a major deficit of this work that should be discussed somewhere, potentially section 4.4.

Reply:

The referee is of course correct, reaction RO_2 + NO leads to alkoxy radicals RO. However, fragmentation is not the only reaction path of RO.

Alkoxy radicals can react with O_2 and under H-abstraction and formation of carbonyl compounds. If the alkoxy radical is a HOM-RO then the product will still contribute to SOA. However, reaction with O_2 is the major path for small peroxy radicals, although Finlayson Pitt and Pitts in their textbook listed substantial branching ratios for this path, p. 190)

RO radicals fragment often by α-scission. In ring systems, like the pinenes, this can lead to ring opening keeping the back bone intact. If the alkoxy radical that breaks apart is a HOM alkoxy and the larger fragment has 7, 8, or 9 C atoms, they could still contribute to SOA formation.

In addition, RO can rearrange very fast by H-abstraction forming an OH group and a radical, which can continue the radical chain. If the H is abstracted from a C atom, O_2 can add to the carbon centered radical and the resulting peroxy radical can continue autoxidation.

If H is abstracted from a hydroperoxide group, then the new peroxy radical will be formed in a unimolecular step. Both rearrangement pathways will contribute to SOA formation.

And autoxidation - maybe in combination with the alkoxy pathway - is fast, as can be seen by the high degree of oxidation of the detected HOM-ON.

The referee is correct that fragmentation of alkoxy radicals could lower the SOA yield, however, although fragmentation occurs this does not affect the condensable mass. This can now be seen in the modified Figure 3. We separated the total HOM into monomers and

accretion products and specified for the monomers the contribution of C_{10} compounds and $C_{<10}$ compounds as $f[NOX]_{SS}$. Figure 3 is limited to a mass range where compounds will condense according to our analysis (section 4.2, Figure 6). We assume that $C_{<10}$ compounds arise mainly from alkoxy radical decomposition. The importance of $C_{<10}$ compounds increases with NO_X, but they must carry more oxygen to get molecular masses larger than 230 Da, i.e.one O atom more per C atom lost. Therefore the $C_{<10}$ compounds will still contribute to the SOA mass. As a consequence, the major reduction of HOM mass at high $[NOX]_{SS}$ is due to the suppression of HOM-ACC, as can be seen in new Figure 3.
Our reference to a next paper dealing with alkoxy radicals in the conclusion section referred to the mechanistic aspects of HOM formation.

Action: We provided an extended Figure 3, and modified and extended the text in section 3.3 accordingly (p.12, line 26 –p.13, line12 in the revised manuscript). We further added text passages to section 4.4 (p.20, line 32 – p.21, line 6, in the revised manuscript) where we discuss the role of fragmentation via alkoxy radicals on HOM and SOA yield. We added one sentence to the conclusion section (p.23, line 23-25, in the revised manuscript).

Additionally, the grammatical errors throughout impede understanding of the manuscript and need significant improvement before publication.

Reply:
We apologize for that many mistakes and typos. We thank the reviewer for the careful reading of the manuscript and for the corrections. We went through the manuscript in order to improve language and grammar.

All in all, this work is novel and of interest to the readers of ACP, so after addressing these major concerns and the other minor technical edits detailed below this manuscript should be suitable for publication.

Page 1, line 33-35: This could also be due to the higher vapor pressure of HOMON relative to similar non-nitrates as you reference on page 17 line 26-27. Consider rewording to make clear you're basing this statement off the results in this paper.

Thanks for that hint. We clarified, that we are referring to our results of effective uptake of HOM-ON (p.1, line 33-35, in the revised manuscript).

Page 2, line 28: "the absence of particles in the presence of NOx": consider rewording. The presence of NOx doesn't mean there's no particles around.

Sentence modified (p.3, line 1-2, in the revised manuscript).

Page 5 line 28 – Page 6 line 7: It would be helpful to include the average or typical concentration of OH more clearly. It is state on Page 6 line 3 but it feels a bit buried and is a single value as opposed to the range stated for O3 and shown for OH in Fig.1. Furthermore, the range of O3 stated on page 5 line 13 does not match that on page 6 line 2. I would suggest adding the O3 and OH concentrations to Table 1.

Table 1 extended as requested.

Page 8, line 10: please justify ignoring wall loss by providing a reference for particle- wall loss rates on similar chambers, or a loss rate estimate from your measurements.

We added a reference to an earlier study: Mentel et al. 2009, lifetime of particles ≈ residence time of air in the chamber.

Page 8, line 25: what is meant by "molecules with finite vapor pressures"? Isn't the vapor pressure finite with a given structure at a given temperature and pressure?

reformulated at both instances

Page 10, line 7-9: is Sp the surface area of the particles? Sentence starting with "Varying Lp(HOM)" is confusing, isn't that relationship linear by definition? Consider rewording to replace the verb "led", similar to the sentence on page 13, lines 11-12.

now: surface area added

We reformulated the passage according the suggestions (p.10, line 25-29, in the revised manuscript)

Page 11 line 16-17: the comment about the endo versus exocyclic bonds should either be explained and/or cited here, or be moved to the discussion section. Fig 2: Should note what these were normalized to as in Figure 4 caption.

Since we are referring to well-known properties of compounds with exocyclic and endocyclic double bonds, we will not move that to discussions. We reformulated the text passage.
The caption of Figure 2 was changed accordingly (p.12, line 7-17, in the revised manuscript)

Page 13 line 11-13: is this based on assumptions or was new particle formation observed? Consider rewording for clarity. Does loss to particles include loss to NPF in the correction?

The formation of new particle does not matter much for the uptake experiments themselves as long as the particle surface area is determined correctly. However, one needs particle free conditions to measure directly the reference c^0(HOM) at the same HOM production rate. The wall loss coefficient L_W can be determined at lower concentrations. Too low c^0(HOM) because of NPF will cause negative intercept in L_P vs. S_P plots like Figure 5. We modified the manuscript and explained more precisely what was done to determine c^0(HOM) despite of NPF during the non-seeded part of the experiment (p.10, line 31 – p.11, line 2, and p.14, line17-22, in the revised manuscript).

Fig 6: why does the C10H16O7-10 vary so much from the C10H14O7-10 & C10H16OxNO2 homologues in that oxygen range? Is it possible that the peaks are mis-assigned or contain multiple compounds? On page 13 line 22 it is stated that: "the potential to condense on particles was about the same for HOM-PP and HOM-ON", however this is not entirely consistent with C10H16O7-10 in Figure 6?

We checked and the peaks are not miss-assigned. And yes, more than one compound can contribute to a given molecular formula. For example, a compound with molecular structure that causes very low vapor pressure could dominate the signal. We added a short discussion of that issue to the manuscript (p.19, line 4-5, in the revised manuscript).

Page 16 paragraph starting line 15: Where does the factor of 1/5 come from? Also, I find the distinction, or lack thereof, of OrgNO3 and ON confusing throughout the manuscript but particularly in this paragraph. Please clearly define the difference somewhere or use the same acronym throughout.

The factor 1/5 is the mass fraction of nitrate (NO_3-, 62 Da) in ON with an average molecular mass of 300 Da. We clarified that.
The referee is correct, there are places where $OrgNO_3$ and ON were mixed. Otherwise $OrgNO_3$ is a terminus technicus used by the AMS community and we would like to stick to it. We defined $OrgNO_3$ clearly in the AMS section, and underlined its importance as diagnostic quantity for linking particulate phase observations and gas-phase observations.
We went through manuscript and tried to clearer distinguish ON and $OrgNO_3$.We added a note to section 2.3 (p.8, line 16-17, in the revised manuscript), reformulated section 4.1. in large parts (p.18 line 2-15, in the revised manuscript) and modified the first paragraph of section 4.2 (p.18, line 22-23, in the revised manuscript).

Page 17 line 4-5 & 7-8: would be helpful to define HOM with respect to # of Oxygens or to define "few O-atoms" with a number. This could be defined on page 3, lines 13-14 or lines 33-34.

We specified the number of Oxygen numbers as requested
We added the definition of HOM in the introduction section (p.4, line 12-13, in the revised manuscript).

Page 18, line 9-10: do you see this higher SOA mass for NOx experiments relative to no-NOx? Has it been reported elsewhere?

This effect will be very difficult to determine. At SOA yields of 10-20% with 50% pON it would be a 1 % effect. It might be overlapped by effects of varying [OH] and the HOM-ACC suppression. It has thus not been reported elsewhere. More importantly, hydrolysis of ON in the particulate phase will probably mask the effect. That is what we tried to address.
We reformulated this part of the manuscript to indicate that the effect would be small (p.19, line 29-31, in the revised manuscript).

Page 18, 1st paragraph section 4.3: can you describe better what Zhao did and do a more complete comparison? As-is, it seems like you're in perfect agreement that 10-11% of the OrgNO3 is in the particle phase, but then lines 18-19 says you're not in agreement?

We added more information of the Zhao experiments (p.20, line 3-7, in the revised manuscript).
Zhao et al. find agreement between expected $OrgNO_3$ from HOM and observation in the particulate phase, whereas in our study we only realized 20-30% of the expected $OrgNO_3$

from HOM in the particulate phase. We expressed clear wherein the studies do agree and do not agree (p.20, line 8-10, in the revised manuscript).

Section 4.4: language could be formalized more throughout this section. “Mass loss” is a somewhat misleading phrase to mean converting potentially condensing species to non-condensable, not a direct loss of SOA mass due to, for example, evaporation. Please rework to be clearer and more streamlined.

Paragraph was reformulated in large parts. The notation mass loss was omitted, where possible. (p.21, line 5 – p. 22, line 8, in the revised manuscript)

page 21 line 12-13: please provide citations

references provided

References

Mentel, T. F., Wildt, J., Kiendler-Scharr, A., Kleist, E., Tillmann, R., Dal Maso, M., Fisseha, R., Hohaus, T., Spahn, H., Uerlings, R., Wegener, R., Griffiths, P. T., Dinar, E., Rudich, Y., and Wahner, A.: Photochemical production of aerosols from real plant emissions, Atmospheric Chemistry and Physics, 9, 4387-4406, 2009

Reply to reviewer #3

We thank the reviewer #3 for the helpful comments. We addressed all points raised.

Anonymous Referee #3

Received and published: 20 March 2020

This manuscript reported HOM organic nitrates, permutation products, and accretion products formation from the oxidation (mostly OH oxidation) of a-pinene and b-pinene. Effective uptake coefficients of HOM on particles was also investigated and reported. Experiments were conducted in CSTR under high RH conditions without seed particles (except for the uptake experiments). It was found that increasing NOx affects the fraction of each type of HOM products formed. The fraction of organic bound nitrate (OrgNO3) stored in gas-phase HOM-ON was found to be substantially higher than the fraction of particulate OrgNO3 and was attributed to particle-phase hydrolysis of OrgNO3. Lastly, SOA yields were also reported and discussed. The suppression of SOA yields with increasing NOx was attributed to suppression of gas-phase HOM accretion products.

This is an interesting study and falls within the scope of ACP. It contributes to our further understanding of monoterpene oxidation in the presence of NOx and the resulting organic nitrate formation and chemistry. There are three main comments that should be addressed prior to publication

1) more analysis needs to be conducted to reconcile the discrepancy between the fraction of particulate OrgNO3 reported in this study and other prior studies in literature. The authors attributed this to hydrolysis but this is not supported by data in literature,

2) more details need to be provided regarding the evaluation of the effective uptake coefficients, and

3) the manuscript should be edited for language. More detailed comments are provided below.

Reply:

1) In contrast to the opinion of referee #3 we are convinced that literature data is in support of our explanations. We would like to note that hydrolysis of ON and particulate ON is not the focus of our paper and our data at one RH are not suited to reconcile possibly inconclusive findings in the literature:

a) Our methodology is sound: because the effective uptake coefficients for both, HOM-PP and HOM-ON are close to unity, we can predict the mass fraction of ON and also organic bound nitrate ($OrgNO_3$) in particles. $OrgNO_3$ expected by uptake of HOM was compared to the amount of $OrgNO_3$ found in the particles by direct measurement. We found a strong discrepancy. A likely explanation for this difference is hydrolysis of organic nitrates in the condensed phase, as this is discussed extensively in the literature (e.g.). The experiments here were performed at 60% RH. Considering the strong dependence of hydrolysis on relative humidity we could also explain the differences of the $OrgNO_3$ content in particles found by us in different experiments at lower relative humidity of 30% (here and Zhao et al., 2018).

b) The production of ON depends on the VOC/NOX ratio and only a fraction of the ON will be transferred to the particulate phase and contribute to SOA. Hydrolyzing of the

particulate phase ON depends on their structure (Boyd et al. 2015, Browne et al. 2013, Hu et al.2011), relative humidity, and the acidity of the particles (Rindelaub et. al. 2015). Hence, the fraction of particulate $OrgNO_3$ in particles can be variable in lab studies at different conditions and a same content of $OrgNO_3$ cannot be expected a priori. This makes comparison between experiments difficult.

c) ON hydrolysis depends on the character of the ON and only tertiary ON are supposed to hydrolyse fast (Hu et al. 2011). The fraction of tertiary ON depends on the formation process. E.g. oxidation of β-pinene with NO_3 led to only a small fraction of tert. ON, so hydrolysis is not so important in case of VOC oxidation by NO_3 (Boyd et al. 2015), whereas photochemical production can lead to large fractions of tert. ON and strong hydrolysis (Browne et al. 2013, Takeuchi and Ng, 2019).

Taking a) - c) into account we come to different conclusions as Referee 3. In contrast to the opinion of referee #3 we assess our results as being well within the range of findings reported in the literature (e.g. Day et al., 2010; Liu et al., 2012; Browne et al., 2013; Jacobs et al., 2014; Rindelaub et al., 2016, 2015; Boyd et al., 2015; Bean and Hildebrandt Ruiz, 2016, Takeuchi and Ng, 2019). All found fast and substantial hydrolysis for photochemically formed particulate ON.

2) We agree with referee #3 that our descriptions of the determination of effective uptake coefficients (Section 2.4) needed some more details on the experiments. This is described in our response to the specific comment 3.b and we accordingly modified section 2.4.

3) We went through the manuscript and removed grammatical errors and tried to improve the language.

Specific comments

1. Page 5 line 12. It would be useful to include the amount of ozone added and the steady state ozone concentration in Table 1.

We modified and extended Table 1.

2. Page 6 line 16. Were the seed particles dried before being injected into the chamber? I would assume not but it is not clear from the manuscript. Please specify.

The particles were dried and this is now described in the experimental section (p.6, line 26, in the revised manuscript)

3. Page 8 section 2.4

a. Line 25. What does “finite vapor pressure” mean?

We reformulated that sentence and skipped the notation finite pressure (p.9, line 17 and line 20, in the revised manuscript).

b. I do not fully understand how these experiments were conducted. From this section, it appears that experiments without seeds (and no organic aerosol formation via nucleation)

were compared with experiments with seeds (ammonium sulfate particles injected) to determine the effective uptake coefficient.

Reply:
No, the uptake experiments were done in one run, starting with the non-seeded chamber. When steady state was reached i.e. stable HOM production, seed particles were added over a few hours to the chamber. Since the chemical production was not affected by adding seed particles, the surface of seed particles provided an increasing sink for the HOM, leading to lower concentrations compared to the non-seeded start. To achieve a sufficient dynamic range of HOM concentrations, a certain level of β-pinene was needed, that caused some NPF in the non-seeded begin of the experiment. The NPF required extrapolation to zero surface in order to calculate c^0(HOM). c^0(HOM) is the concentration in absence of particles which is only determined by (same) production and wall loss. The wall loss coefficients of HOM were determined in independent experiments at lower concentration levels.
We reformulated section 2.4 to better describe how the experiments were conducted. A short paragraph was put in front of Section 2.4 where the experimental procedure is shortly described (p. 9, line 1-8, in the revised manuscript).

My understanding from the experimental section is that seed particles were only added in "experiment series 3" (i.e., experiments to determine effective uptake coefficient), and no seed particles were added in all other experiments. Presumably, organic aerosol formation via nucleation took place in all other experiments. However, according to Table 1, the b-pinene mixing ratio used in "experiment series 3" was the same as other all experiments. If so, shouldn't nucleation also took place in ""experiment series 3", and that particles (organic particles) would be present in the system even though no ammonium sulfate particles were added (see page 13 line 12)? If this is the case, one needs to consider uptake onto pure organic particles? Please describe and discuss these clearly in the revised manuscript.

Reply:
Yes, the referee is correct, seed particles were added only in experiment series 3. Regarding the effects of NPF in determining y_{eff}: uptake of HOM by pure organic particles was certainly considered. The surface concentration (S_P) of purely organic particles was $0.2x10^{-3}$ m^2/m^3 while S_P increased up to $1.2x10^{-3}$ m^2/m^3 after adding seeds. Plots 1/c(HOM) vs. S_P where linear over the whole range. Or in other words, the pure organic particles matched the behavior of the coated ones. To make this clearer we modified section 2.4 and added a short paragraph in Section 2.4 (p 9, line 1-8, p.10, line 24 - 31 and p.11, line 1-2, in the revised manuscript).
We discussed the procedure of determining γ_{eff} also section 3.5 (p.14, line17-22, in the revised manuscript)

Particle formation by NPF was desired in experiment series 4 in order to determine $OrgNO_3$ by AMS. The experiments were started at low NO_X to get nucleation and then NO_X was stepwise increased. This seemed easier to us in organic aerosols than in aerosols with seeds. Since HOM form SOA by solely condensation, the organic matrix is the same in SOA formed in NPF and on neutral ammonium sulfate seeds. As stated, the resulting SOA yields shown in Figure 7 were about the same as yields observed in seeded experiments in Sarrafzadeh et al. 2016. In experiment 1 NPF wouldn't affect the results, but in presence of NO_X NPF is strongly suppressed anyhow (Wildt et al., 2014, Sarrafzadeh et al., 2016). So,

NPF is only unwanted in experiment series 2, where one would like to have the HOM totally in the gas-phase in order to determine the expected composition of the SOA by HOM-PP, HOM-ON, HOM-ACC. In the low NO_X cases some NPF took place in series 2, but again with increasing NO_X NPF was suppressed. In cases where NPF took place, loss to particles was corrected as described in supplement section S3.

4. Page 12, line 12. The authors noted that the highly-oxidized C<10 nitrates were observed with increasing NOx and that "supposedly, they did not arise from gas-phase chemistry but were formed at the walls". Please elaborate. What mechanisms at the walls? If there is chemistry on the walls, how would this affect section 2.4 (determination of uptake coefficient) if there is also some sort of wall memory?

As described in manuscript, these compounds had a different composition and showed a different time behavior (increased with time independent on the photochemistry). They cannot affect the uptake coefficients, because the uptake coefficients were determined at $[NOX]_{SS}$ = 4 ppb (β-pinene) or less (α-pinene). As stated in the manuscript and can be seen in Figure S5 (supplement) at these NO_X levels such compounds were unimportant. They could have some effect on the SOA yields at the highest NO_X, but that effect is at maximum their contribution to the total HOM. The chamber was flushed for at least on day between experiments until the compounds were below detection limit.
We believe that we gave the phenomenon sufficient attention and showed that it does not much affect our results.
We further weakened the statement that they are formed at the wall (p.14, line 6-8, in the revised manuscript).

5. Page 13, line 16, please also indicate (e.g., in Figure 7) the organic mass concentration, as SOA yield is also highly dependent on organic mass.

We don't understand this comment. The paragraph at page 13 around line 16 deals with uptake coefficients and Figure 5. We are of course aware that SOA yields depend on OA mass, but this not our question here. Experiments in Figure 7 where all performed at the same conditions but changing NO_X. The average SOA load was 16±5 μg/m^3, ranging from 11 μg/m^3 to 23 μg/m^3 and this information was added to the caption of Figure 7, in the revised manuscript.

6. Page 14, lines 1-2. Are these mass concentrations in the gas and particle phases consistent with equilibrium partitioning of HNO3?

Reply:
We obviously did not specify sufficiently what we meant. We modified the text (p.15, line 9-11, in the revised manuscript).
Equilibrium partitioning of HNO_3 is difficult to predict for SOA at 60%RH. There is some water in the particles and the system will be highly non-ideal. In any case at 24 ug/m^3 HNO_3 (<8 ppb) the amount in the particulate phase will be orders of magnitude smaller than the gas-phase concentration and an upper limit of 0.1 ug/m^3 is well within expectations by thermodynamics. (HNO_3 has a vapor pressure at RT of about 5000 Pa.) However, for our considerations it is only important that we determined the $OrgNO_3$ mass correctly and do not falsely count $OrgNO_3$ as inorganic nitrate.

7. Page 16, line 9. There are many more studies. For example, see review and references in Ng et al. (ACP, 2017). Some more recent studies, for example, Claflin and Ziemann (J. Phys. Chem. A, 2018), are also relevant.

We added more references including Ng et al., 2017, as well as Claflin and Ziemann, 2018,

8. Page 16 line 16. A recent study by Takeuchi and Ng (ACP, 2019) also reported on the ON formed by photooxidation of monoterpenes.

We added Takeuchi and Ng, 2019 to the reference list.

9. Page 16 line 23. Please provide citations for this statement "We found contributions between 0 % and 2.7 % by AMS, which is within the range of most other data reported in the literature but at the lower end.".

We modified that passage and added references. (p.17, line 5-16, in the revised manuscript)

10. Page 17 line 9. It was stated that "Our findings are in agreement with observations by Lee et al. (2016b) in a field study." My understanding is that the study by Lee et al. was conducted in a rural environment, presumably with very low level of NOx. The ambient conditions were quite different from laboratory conditions employed in this study. Please justify why an agreement would be expected between results in Lee et al. and this study.

We specified more clearly what we are going to compare (p.18, line 25-26, in the revised manuscript).

11. Page 18-19, section 4.3. The fraction of OrgNO3 is much lower in this study than Zhao et al. and other studies in literature. The authors attributed this to potential hydrolysis of organic nitrates in the particle phase as experiments in Zhao et al. were conducted at much lower RH. However, a recent study by Takeuchi and Ng (ACP,2019), conducted at similar RH to this study, showed that the fraction of organic nitrates in the particles is also much higher than that reported in this study, and the fraction or organic nitrates undergoing hydrolysis was constrained. More analysis should be conducted here to evaluate why the value reported in this study is much lower than prior literature.

Reply
We think there is a misunderstanding. $OrgNO_3$ is not the same as particulate ON. It is the nitrate carried by ON. We clarified that throughout the manuscript. We added a note to section 2.3 (p.8, line 16-17, in the revised manuscript), reformulated section 4.1. in large parts (p.18 line 2-15, in the revised manuscript) and modified the first paragraph of section 4.2 (p.18, line 22-23, in the revised manuscript).
We basically show that HOM will dominate the composition of particulate phase in our experiment, because of their large γ_{eff}. Therefore we can predict from the HOM composition, i.e. HOM-PP, HOM-ON and HOM-ACC, the ON and therewith $OrgNO_3$ that should be expected in the particulate phase. We modified the text at several instances showing and discussing now mass concentrations of HOM-ON and all other HOM in new Figure 3 and

new Figure 4. From new Figures 3 and 4 it should now become clear that we got ON mass fractions up to several 10% in the particulate phase. This is in agreement with many other studies, including Takeuchi and Ng, 2019. The discrepancy we discussed was in OrgNO_3 expected from HOM and directly measured by AMS, where we find 60-80% loss of the nitrate function. This is somewhat higher than observations of Takeuchi and Ng, 2019, but in agreement with expectations discussed in Boyd et al., 2015, Browne et al. 2013, Fisher et al., 2016.

References

Boyd, C. M., Sanchez, J., Xu, L., Eugene, A. J., Nah, T., Tuet, W. Y., Guzman, M. I., and Ng, N. L.: Secondary organic aerosol formation from the β-pinene+NO_3 system: effect of humidity and peroxy radical fate, Atmos. Chem. Phys., 15, 7497-7522, 10.5194/acp-15-7497-2015, 2015.

Browne, E. C., Min, K. E., Wooldridge, P. J., Apel, E., Blake, D. R., Brune, W. H., Cantrell, C. A., Cubison, M. J., Diskin, G. S., Jimenez, J. L., Weinheimer, A. J., Wennberg, P. O., Wisthaler, A., and Cohen, R. C.: Observations of total $RONO_2$ over the boreal forest: NO_x sinks and HNO₃ sources, Atmos. Chem. Phys., 13, 4543-4562, 10.5194/acp-13-4543-2013, 2013.

Claflin, M. S., and Ziemann, P. J.: Identification and Quantitation of Aerosol Products of the Reaction of beta-Pinene with NO_3 Radicals and Implications for Gas- and Particle-Phase Reaction Mechanisms, Journal of Physical Chemistry A, 122, 3640-3652, 10.1021/acs.jpca.8b00692, 2018.

Fisher, J. A., Jacob, D. J., Travis, K. R., Kim, P. S., Marais, E. A., Chan Miller, C., Yu, K., Zhu, L., Yantosca, R. M., Sulprizio, M. P., Mao, J., Wennberg, P. O., Crounse, J. D., Teng, A. P., Nguyen, T. B., St. Clair, J. M., Cohen, R. C., Romer, P., Nault, B. A., Wooldridge, P. J., Jimenez, J. L., Campuzano-Jost, P., Day, D. A., Hu, W., Shepson, P. B., Xiong, F., Blake, D. R., Goldstein, A. H., Misztal, P. K., Hanisco, T. F., Wolfe, G. M., Ryerson, T. B., Wisthaler, A., and Mikoviny, T.: Organic nitrate chemistry and its implications for nitrogen budgets in an isoprene- and monoterpene-rich atmosphere: constraints from aircraft (SEAC4RS) and ground-based (SOAS) observations in the Southeast US, Atmos. Chem. Phys., 16, 5969-5991, 10.5194/acp-16-5969-2016, 2016

Hu, K. S., Darer, A. I., and Elrod, M. J.: Thermodynamics and kinetics of the hydrolysis of atmospherically relevant organonitrates and organosulfates, Atmos. Chem. and Phys., 11, 8307-8320, 10.5194/acp-11-8307-2011, 2011.

Rindelaub, J. D., McAvey, K. M., and Shepson, P. B.: The photochemical production of organic nitrates from alpha-pinene and loss via acid-dependent particle phase hydrolysis, Atmos. Environ., 100, 193-201, 10.1016/j.atmosenv.2014.11.010, 2015

Takeuchi, M., and Ng, N. L.: Chemical composition and hydrolysis of organic nitrate aerosol formed from hydroxyl and nitrate radical oxidation of α-pinene and β-pinene, Atmos. Chem. Phys., 19, 12749-12766, 10.5194/acp-19-12749-2019, 2019

Impact of NO_x on secondary organic aerosol (SOA) formation from α-pinene and β-pinene photo-oxidation: the role of highly oxygenated organic nitrates

Iida Pullinen[1,4], Sebastian Schmitt[1,5], Sungah Kang[1], Mehrnaz Sarrafzadeh[1,3,6], Patrick Schlag[1,7], Stefanie Andres[1], Einhard Kleist[2], Thomas F. Mentel[1], Franz Rohrer[1], Monika Springer[1], Ralf Tillmann[1], Jürgen Wildt[1,2], Cheng Wu[1,8], Defeng Zhao[1,9], Andreas Wahner[1] and Astrid Kiendler-Scharr[1]

[1]Institute for Energy and Climate Research, IEK-8, Forschungszentrum Jülich, 52425, Jülich, Germany
[2]Institute of Bio- and Geosciences, IBG-2, Forschungszentrum Jülich, 52425, Jülich, Germany
[3]Centre for Atmospheric Chemistry, York University, 4700 Keele St., Toronto, ON M3J 1P3, Canada
[4]Present address: Department of Applied Physics, University of Eastern Finland, Kuopio, Finland
[5]Present address: TSI GmbH, 52068 Aachen, Germany
[6]Present address: PerkinElmer, 501 Rowntree Dairy Rd, Woodbridge, ON, L4L 8H1, Canada
[7]Present address: Shimadzu Deutschland GmbH, 47269 Duisburg, Germany
[8]Present address: Department of Environmental Science, Stockholm University, 11418 Stockholm, Sweden
[9]Present address: Dept. of Atmos. and Oceanic Sci. & Inst. of Atmos. Sci., Fudan University, Shanghai, 200438, China

Correspondence to: Thomas F. Mentel (t.mentel@fz-juelich.de)

Abstract. The formation of organic nitrates (ON) in the gas phase and their impact on mass formation of Secondary Organic Aerosol (SOA) was investigated in a laboratory study for α-pinene and β-pinene photo-oxidation. Focus was the elucidation of those mechanisms that cause the often observed suppression of SOA mass formation by NO_x, and therein the role of highly oxygenated multifunctional molecules (HOM). We observed that with increasing NO_X a) the portion of HOM organic nitrates (HOM-ON) increased, b) the fraction of accretion products (HOM-ACC) decreased and c) HOM-ACC contained on average smaller carbon numbers.

Specifically, we investigated HOM organic nitrates (HOM-ON), arising from the termination reactions of HOM peroxy radicals with NO_x, and HOM permutation products (HOM-PP), such as ketones, alcohols or hydroperoxides, formed by other termination reactions. Effective uptake coefficients γ_{eff} of HOM on particles were determined. HOM with more than 6 O-atoms efficiently condensed on particles (γ_{eff} > 0.5 in average) and for HOM containing more than 8 O-atoms, every collision led to loss. There was no systematic difference in γ_{eff} for HOM-ON and HOM-PP arising from the same HOM peroxy radicals. This similarity is attributed to the multifunctional character of the HOM: as functional groups in HOM arising from the same precursor HOM peroxy radical are identical, vapor pressures should not strongly depend on the character the final termination group. As a consequence, the suppressing effect of NO_X on SOA formation cannot be simply explained by replacement of terminal functional groups by organic nitrate groups.

According to their γ_{eff} all HOM-ON with more than 6 O-atoms will contribute to organic bound nitrate ($OrgNO_3$) in the particulate phase. However, the fraction of $OrgNO_3$ stored in condensable HOM with molecular masses >230 Da appeared to be substantially higher than the fraction of particulate $OrgNO_3$ observed by aerosol mass spectrometry. This result suggests

losses of $OrgNO_3$ for organic nitrates in particles, probably due to hydrolysis of $OrgNO_3$ that releases HNO_3 into the gas phase but leaves behind the organic rest in the particulate phase. However, the loss of HNO_3 alone, could not explain the observed suppressing effect of NO_X on particle mass formation from α-pinene and β-pinene.

Instead we can attribute most of the reduction in SOA mass yields with increasing NO_X to the significant suppression of gas-phase HOM-ACC which have high molecular mass and are potentially important for SOA mass formation at low NO_X conditions.

1 Introduction

Secondary organic aerosol (SOA) constitutes a substantial fraction of ambient aerosol. It is formed from oxidation products of volatile organic compounds (VOC) and known to adversely affect visibility, climate and human health (Hallquist et al., 2009). With annual emissions around 1100 Tg, the biosphere is the strongest source of tropospheric VOC (Guenther et al., 2012) and thus, SOA formation from biogenic VOC is of high importance. Despite the outstanding role of biogenic VOC by amount and reactivity, anthropogenic trace gases affect SOA formation and possible anthropogenic enhancement effects were found in laboratory and field studies (e.g., Carlton et al., 2010; De Gouw et al., 2005; Emanuelsson et al., 2013; Glasius et al., 2011; Hoyle et al., 2011; Shilling et al., 2013; Spracklen et al., 2011; Worton et al., 2011; Xu et al., 2015a) Examples of important anthropogenic trace gases are NO and NO_2, which together form the NO_X family. During nighttime NO_X is converted to NO_3 radicals, which oxidize biogenic VOC, leading to organic nitrates and SOA formation (Boyd et al., 2017; Boyd et al., 2015; Claflin and Ziemann, 2018; Faxon et al., 2018; Fry et al., 2013, 2014; Kiendler-Scharr et al., 2016; Lee et al., 2016a; Ng et al., 2017). During daytime, NO_X controls the atmospheric HO_X cycle thus the oxidation cycle of VOC by reaction with peroxy radicals. In this study we will focus on role of NO_X for SOA formation during daytime. In a number of studies the role of NO_X in the formation of SOA mass was investigated (Eddingsaas et al., 2012; Han et al., 2016; Kim et al., 2012; Kroll et al., 2006; Lee et al., 2016a; Lee et al., 2020; Ng et al., 2007; Pandis et al., 1991; Presto et al., 2005; Rindelaub et al., 2015, 2016; Sarrafzadeh et al., 2016; Stirnweis et al., 2017; Zhang et al., 2006). In most cases it was observed that NO_X decreased mass yields of SOA formation and the effects were generally attributed to impacts of RO_2 + NO reactions. Sarrafzadeh et al. (2016) show that parts of the apparent suppression of SOA yields from β-pinene by NO_X was due to the role of NO_X in the HO_X cycle. As mass yields of SOA formation from α-pinene and β-pinene photo-oxidation depend on the actual OH concentrations, NO_X affects SOA formation also via decreasing or increasing OH concentrations according to reactions R1 and R2:

$$OH\cdot + NO_2 + M \rightarrow HNO_3 + M \quad (R1)$$

$$HO_2\cdot + NO \rightarrow OH\cdot + NO_2 \quad (R2)$$

NO_X is inhibiting new particle formation (NPF, Wildt et al., 2014), therefore, in absence of seed particles, NO_X can prevent formation of sufficient particle surface where low volatile compounds could condense on. In absence of particles other sinks gain in importance for low volatile compounds as dry deposition in the environment or wall losses in chamber experiments. In order to circumvent these effects, Sarrafzadeh et al. (2016) used seed particles always providing sufficient surface for the gas phase precursors of SOA mass to condense on and kept the OH concentrations constant. As a result the remaining effect of NO_X on SOA mass formation from β-pinene and on SOA yields was only moderate. Generally, in absence of NO_X, peroxy radicals (RO_2·) mainly react with other peroxy radicals (including the HO_2· radical) whereby termination products like hydroperoxides, ketones, alcohols, carboxlic acids and percarboxylic acids are produced. In reactions between peroxy radicals also alkoxy radicals are formed, which continue the radical chain (R4b):

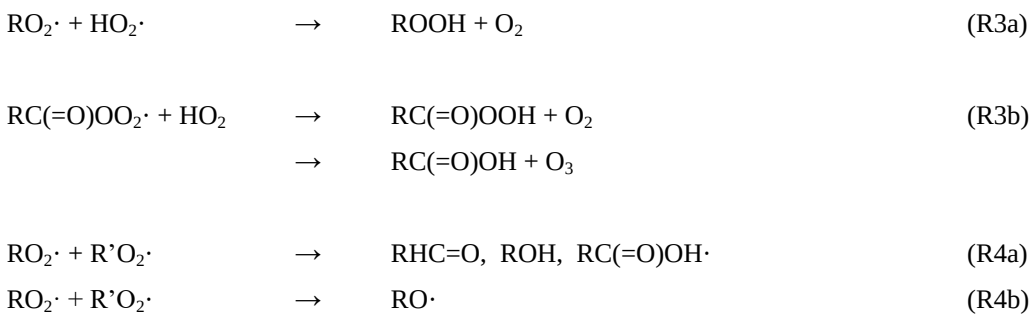

$$RO_2\cdot + HO_2\cdot \rightarrow ROOH + O_2 \quad (R3a)$$

$$RC(=O)OO_2\cdot + HO_2 \rightarrow RC(=O)OOH + O_2 \quad (R3b)$$
$$\rightarrow RC(=O)OH + O_3$$

$$RO_2\cdot + R'O_2\cdot \rightarrow RHC=O,\ ROH,\ RC(=O)OH\cdot \quad (R4a)$$
$$RO_2\cdot + R'O_2\cdot \rightarrow RO\cdot \quad (R4b)$$

As observed in several studies with highly oxygenated multifunctional organic molecules (HOM, e.g. Berndt et al., 2018a, b; Ehn et al., 2012; Ehn et al., 2014; Mentel et al., 2015;) accretion products can be formed in peroxy - peroxy radical reactions:

$$RO_2\cdot + R'O_2 \rightarrow ROOR' + O_2 \quad (R5)$$

In laboratory studies HOM accretion products can contribute significantly to SOA yields (McFiggans et al., 2019).

The presence of NO_X opens new pathways with large reaction rates and production of organic nitrates (R6a), including PAN-like compounds (R7). Furthermore, substantial amounts of alkoxy radicals (R6b) are formed:

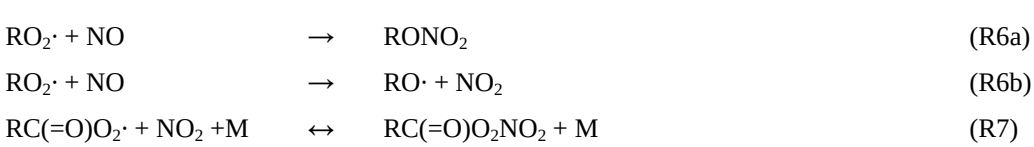

$$RO_2\cdot + NO \rightarrow RONO_2 \quad (R6a)$$
$$RO_2\cdot + NO \rightarrow RO\cdot + NO_2 \quad (R6b)$$
$$RC(=O)O_2\cdot + NO_2 + M \leftrightarrow RC(=O)O_2NO_2 + M \quad (R7)$$

From reactions R3 to R7 it is obvious that the chemically stable products of peroxy radicals will have different termination groups under low and high NO_X conditions: while hydroperoxides, ketones, carboxylic acids etc. predominate at low NO_X conditions, organic nitrates (ON), including PAN like compounds become more important at high NO_X conditions.

Recent studies demonstrated the dominant role of HOM in SOA mass formation (Ehn et al., 2014; Jokinen et al., 2015; McFiggans et al., 2019; Mutzel et al., 2015; Zhang et al., 2017). HOM are formed by addition of molecular oxygen to alkyl radicals that are formed after H-migration in peroxy- or in alkoxy radicals. Due to a relative long lifetime of peroxy radicals such H-shifts with addition of molecular oxygen can appear several times in sequential steps and is therefore termed autoxidation (Crounse et al., 2011; Mentel et al., 2015; Rissanen et al., 2014). This process leads to highly oxygenated multifunctional peroxy radicals (HOM peroxy radicals). If the respective HOM is formed exclusively via autoxidation of peroxy radicals, the HOM moieties are very likely multiple hydroperoxides (Berndt et al., 2016; Rissanen et al., 2014). If there are intermediate steps via alkoxy radicals there maybe also alcohol groups (Mentel et al., 2015). Bianchi et al. (2019) suggested using the notation HOM when the autoxidation products carry six or more O-atoms.

HOM are low volatile organic compounds (LVOC) or even extremely low volatile organic compounds (ELVOC) and they substantially contribute to mass formation of particles and support NPF (; Bianchi et al., 2016; Ehn et al., 2014; Kirkby et al., 2016; Lehtipalo et al., 2018; Tröstl et al., 2016). All experimental evidence show that HOM peroxy radicals terminate with similar rates as less functionalized peroxy radicals (Berndt et al., 2016; Bianchi et al., 2019; Ehn et al., 2017). At low NO_X levels, HOM hydroperoxides, HOM alcohols, HOM carboxylic acids and HOM percarboxylic acids as well as HOM ketones are expected from the termination step and in addition HOM accretion products (HOM-ACC).

At high NO_X levels HOM-ON become important termination products. In addition HOM-ACC products are suppressed (Lehtipalo et al., 2018) and shifted to smaller C-numbers. The effect of NO_X on HOM-RO_2 chemistry is important step for understanding of impact of NO_X on SOA formation. In this paper we analyze two aspects of the effect of NO_X which are important for SOA yield: the formation and the volatility of HOM-ON as well as the suppression of HOM accretion products.

2 Experimental

2.1 Description of the chamber setup and experiments

Experiments were conducted in the Jülich Plant Atmosphere Chamber (JPAC, Mentel et al., 2009; 2013). The actual setup of the chambers was already described in several recent publications (Ehn et al., 2014; Mentel et al., 2015; Sarrafzadeh et al., 2016; Wildt et al., 2014). A 1.45 m^3 chamber made of borosilicate glass and set up in a climate-controlled housing was used for these experiments. The chamber was operated as a continuously stirred tank reactor. About thirty-one liters of purified air per minute were pumped through the chamber resulting in a residence time of approximately 46 min. Mixing was ensured by a fan and the mixing time was about 2 minutes. The inlet flow was provided by two about equal purified air streams with one of them containing ozone and water vapor. In the second stream the VOC of interest was introduced from a diffusion

source. Temperature (16 ± 1 °C) and relative humidity (63 ± 2%) inside the chamber were held constant over the course of the experiments.

The chamber was equipped with several lamps. Two discharge lamps (HQI400 W/D, Osram) served to simulate the solar light spectrum. Twelve UVA discharge lamps (Philips, TL 60 W/10-R, 60W, λ_{max} =365 nm) provided the photolysis of NO_2 with a photolysis frequency $J(NO_2)$ of ~3.3×10^{-3} s^{-1}. An UVC lamp (Philips, TUV 40W, λ_{max} =254 nm) was used to produce OH radicals by ozone photolysis and reaction of O^1D atoms with water vapor. This lamp was housed in a quartz tube across the chamber diameter and parts of the lamp were shielded by movable glass tubes. By altering the gap between these glass tubes, the photolysis frequency for ozone, $J(O^1D)$ and therewith the OH production rate could be adjusted. During most of the experiments described here, $J(O^1D)$ was about 2.9×10^{-3} s^{-1}. The photolysis frequencies $J(NO_2)$ and $J(O^1D)$ (as function of the TUV gap) were determined experimentally by actinometry with NO_2 and O_3 in the chamber. Gas-phase compounds were measured such as ozone (O_3, UV-absorption, Thermo Environmental 49), nitrogen monoxide (NO, chemiluminescence, Eco Physics, CLD 770 AL ppt), and nitrogen dioxide (NO_2, chemiluminescence after photolysis, Eco Physics, PLC 760). Water vapor concentrations were measured by dew point mirror (TP- 2, Walz).

We used the monoterpenes α-pinene and β-pinene (both Aldrich, 95% purity) as SOA precursors. The monoterpenes (MT) were measured either by gas chromatography mass spectrometry (GC-MS; Agilent GC-MSD system with HP6890 GC and 5973 MSD) or by proton transfer reaction mass spectrometry (PTR-MS; Ionicon, Innsbruck, Austria). Both devices were switched between the outlet and the inlet of the chamber in order to quantify concentrations in the chamber and to determine the VOC source strength.

To provide NO_X to the photochemical system we added NO_2 (Linde, 100 ppm NO_2 in nitrogen) in the *β*-pinene experiments or NO (90 ppm in nitrogen) in the *α*-pinene experiments to the VOC containing air stream. In case of NO_2 addition, a fraction of the added NO_2 was converted to NO due to the NO_2 photolysis. In case of NO addition, the major portion of the added NO was converted to NO_2 by reaction with O_3. We adjusted the O_3 addition such that a steady state $[O_3]$ within a range of 60 - 90 ppb was achieved. We observed memory effects for NO_X probably due to Teflon parts (tubing, fan) in the chamber. In particular after experiments at high NO_X concentrations residual NO_X appeared in the chamber on the next day when switching on the TUV lamp. To minimize the memory effect, the chamber was operated without NO_X for one day between the NO_X experiments. The background NO_X concentration was around 300 ppt. When adding NO_X, its initial concentration, $[NO_X]_0$ was between 5 and 150 ppb and thus substantially above the background levels.

The results presented here were obtained at steady state conditions when all physical and chemical parameters were constant or in steady state, respectively. To indicate reference to steady state we mark the concentrations of MT and NO_X with the subscript “SS”. To allow better comparison to literature data we refer in some instances to the initial concentrations $[NO_X]_0$, $[\alpha\text{-pinene}]_0$, and $[\beta\text{-pinene}]_0$, indicated by subscript “0”, which are in our case input concentrations.

The OH concentrations were calculated from the decay of the respective MT in the chamber (Eq.2).

$$\frac{d[VOC]}{dt} = \frac{F}{V}([VOC]_0 - [VOC]) - (k_{OH} \cdot [OH] + k_{O3} \cdot [O_3]) \cdot [VOC] \quad (1)$$

$$[OH]_{SS} = \frac{\frac{F}{V}\frac{[VOC]_0 - [VOC]_{SS}}{[VOC]_{SS}} - k_{O3} \cdot [O_3]_{SS}}{k_{OH}} \quad (2)$$

Equation (1) describes mass balance of the MT in the chamber and Eq. (2) results from Eq. (1) under steady state conditions when d[VOC]/dt = 0. In Eq. (1) and (2), V is the volume of the chamber, F is the total air flow through the chamber, $[VOC]_0$ and [VOC] are the concentrations of the VOC under investigation in the inlet air and in the chamber, respectively. k_{OH} and k_{O3} are the respective rate coefficients for the reactions of the VOC with OH and with O_3. In one case, where the concentration of β-pinene was altered during the experiment, m-xylene was added as a tracer for [OH].

Rate constants used for the determinations of [OH] were: k_{OH} = 5.37×10^{-11}, 7.89×10^{-11}, and 2.3×10^{-11} cm^{-3} s^{-1} for α-pinene, β-pinene, and m-xylene, respectively (Atkinson, 1994; Atkinson, 1997). At typical conditions with [O_3] ~ 60-100 ppb and [OH] ~ 3×10^7 the consumption of α-pinene by O_3 (k_{O3} = 8.7×10^{-17} cm^3 s^{-1}) was about 5% compared to that by OH. α-pinene losses due to ozonolysis were therefore neglected for the determination of [OH]. As β-pinene has an even lower ozonolysis rate constant (k_{O3} =1.5×10^{-17} cm^3 s^{-1}, Atkinson, 1997), and m-xylene does not react with O_3 (k_{O3} < 1.5×10^{-21} cm^3 s^{-1}, Atkinson et al., 1994) ozonolysis reactions were also neglected for OH estimations using these VOC. The overall uncertainty in OH concentration was estimated to be about 20% (Wildt et al., 2014).

Our results were obtained in different types of experiments. An overview of the performed experiments with their starting conditions is given in Table 1. Details of the procedures applied during individual experiments are described in the respective sections. Three experiment series (1-3) were conducted to characterize gas phase products and experiment series 4 was conducted to characterize the particle phase. In the first experiment we estimated the molar yield of all organic nitrates (ON) independent of their contribution to particle formation. This was made at the example of β-pinene at one NO_X concentration (see section 3.1). Experiment series 2 were performed to determine the fraction of HOM organic nitrates at the total amount of HOM. Both monoterpenes were used with several NO_X levels as indicated (see section 3.3). In experiment series 3 we determined effective uptake coefficients for HOM at a low and at a high NO_X level for HOM-ON and other HOM termination products (see section 3.4). These experiments were performed with seed particles (ammonium sulfate), which were dried by a silica gel diffusion dryer to RH < 30% before they entered the chamber. In the last experiment series 4 we characterised the amount of nitrate bound to organics in particles for comparison with the amount of organic bound nitrate in those HOM-ON that efficiently contribute to particle formation.

2.2 Determination of highly oxygenated molecules (HOM)

Highly Oxygenated Molecules (HOM) were measured by a Chemical Ionisation Mass Spectrometer operated with nitrate as reagent ion (NO_3^--CIMS, Jokinen et al., 2012). First we determined that the relative transmission curve of our NO_3^--CIMS

was flat (supplement section S1.1). This indicates that detection of HOM within the mass range from ~230 Da to ~600 Da is nearly mass independent. So far, no absolute calibration method exists for HOM. However, the charging efficiency for HOM is near to the kinetic limit like that for sulfuric acid (Ehn et al., 2014; Kirkby et al., 2016). Thus, the sensitivity of the NO_3^--CIMS to HOM is supposedly similar to that of sulfuric acid. We therefore calibrated our NO_3^--CIMS to sulfuric acid and used the calibration coefficient for the HOM, too (see supplement section S1.2). Applying the sulfuric acid calibration coefficient to the HOM we investigated the mass balance between condensable HOM and formed particle mass which was closed within a factor of 2 (see supplement section S1.3). It is also likely that the sensitivity of the NO_3^--CIMS does not depend much on the functional group formed in the final termination step. This assumption is reasonable as HOM formed by autoxidation contain several hydroperoxy groups or a mixture of hydroxy and hydroperoxy groups, if they are formed via the alkoxy peroxy path (Mentel et al., 2015). Furthermore, a good agreement of the fraction of organic nitrates on the total reaction products of β-pinene (see section 3.1) and the fraction of HOM-ON of the total HOM gives us confidence that the uncertainty induced by this assumption does not affect much the main conclusions.

This all together with the quantum mechanical results of same sensitivity for HOM containing 6 or more O-atoms (Hyttinen et al., 2017) gave us confidence that concentrations of HOM with 6 or more O atoms were determined with the same sensitivity to an uncertainty of less than a factor of two.

In summary, we used the calibration coefficient for H_2SO_4 to calculate HOM concentrations. We further concluded a same sensitivity for the detection of all HOM including accretion products when they contained 6 and more O-atoms. These conclusions are supported by observations of Breitenlechner et al. (2017) who found that, once the HOM contains more than 5 O-atoms, the sensitivity is to a good approximation independent of the number of O-atoms. The sensitivity of the NO_3^--CIMS is unclear for compounds containing less than 5 O-atoms (Hyttinen et al., 2017; Rissanen et al., 2014; Riva et al., 2019). However, as will be shown in section 3.4, HOM with less than 5 O atoms are of minor importance for particle mass formation, hence we will neglect them and this will not contribute much uncertainty on our results.

Identification of molecular formulas for individual HOM was obtained using high resolution spectra (resolution power ≈4000) as described in the supplement section S2. In case of HOM spectra from β-pinene photo-oxidation we found many not-fully-resolved double peaks from the overlapping of C_{10}, C_9, and C_8 progressions. The mass spectra of α-pinene HOM in general consisted of singular peaks, i.e. they were quite well resolved. Figure S5 in supplement section S2 shows, how HOM-RO_2 and HOM-ON were separated with increasing NO_X. In the high resolution analysis of α-pinene we focus on the mass range 230 Da to 550 Da. The lower limit 230 Da was chosen because of the equal sensitivity of the NO_3^--CIMS towards HOM as discussed before and because C_{10} compounds with 6 or more O atoms have molecular weights > 230 Da. As we will show in section 4.2 they are LVOC and ELVOC and will contribute to SOA formation. The upper limit was set to 550 Da to reduce the influence of noise since not much signal is found for molecular masses > 550 Da.

The observed concentration of gas-phase HOM depends on the OH concentration and the condensation sink provided by newly forming particles. Adding to or removing NO_X from a given photochemical system directly impacts [OH] by reactions

R1 and R2. NO_X furthermore suppresses new particle formation (Wildt et al., 2014) which leads to a decreasing condensation sink for HOM with increasing NO_X. The actual OH concentration affects the actual turnover of the precursor, thus the actual production of $RO_2\cdot$ and HOM, while the actual condensational sink leads to condensational loss of HOM. Both factors change the observed HOM gas-phase mixing ratio and can superimpose the impacts of NO_X on peroxy radical chemistry itself. In order to separate the chemical impacts of NO_X on HOM peroxy radical chemistry, we needed to take out the effects of [OH] and condensational sink as much as possible. This was achieved by normalizing the HOM mixing ratio to particle free conditions and to a certain reference oxidation rate. The procedure is described in detail in supplement section S3.

2.3 Particle-phase measurements

To characterize the particle phase we used a condensation particle counter (CPC, TSI 3783), a scanning mobility particle sizer (Electrostatic classifier TSI 3080, including a differential mobility analyzer TSI 3081 and a CPC TSI 3025A) and an aerosol mass spectrometer (AMS, Aerodyne HR-ToF-MS, modified for application on a Zeppelin airship, (Rubach, 2013)). In the AMS the aerosol particles were vaporized at 600 ºC and ionized by electron impact ionization at 70 eV. The AMS was routinely operated in V-mode in two alternating modes: 1 min. MS mode to measure the chemical composition and 2 min. PToF mode. Only MS mode data were analyzed here. In the following we will use the amount of nitrate bound to organics ($OrgNO_3$) as a diagnostic to link observation of HOM-ON in the gas-phase to observations in the particulate phase. We separated organic and inorganic particulate nitrate and determined the amount of $OrgNO_3$ by the NO_2^+/NO^+ method for AMS (Farmer et al., 2010; Kiendler-Scharr et al., 2016).

SOA yields were determined as described in Sarrafzadeh et al. (2016). For determining mass yields, the particle mass formed during steady state conditions was divided by the mass of the consumed MT, which is the difference between inlet and outlet concentration:

$$Y = \frac{produced\ particle\ mass}{BVOC\ consumption} \quad (3)$$

During measurements of particle mass, the mean diameter of particles was above 100 nm. As the loss rates of such particles on the chamber walls were low (Mentel et al., 2009), they were neglected. Losses of oxidized SOA precursors to the chamber walls were considered by applying the correction function given by Sarrafzadeh et al. (2016). This function describes the ratio of wall losses over the sum of wall losses and losses on particles. For the data given here, the correction factors were between 1.5 and 2.1.

2.4 Determination of effective uptake coefficients

The experiments to determine effective uptake coefficients for HOM, γ_{eff}, were performed as follows: Signal intensities of the respective HOM were measured at zero (α-pinene) or low particle load (β-pinene). Then we introduced dried seed particles into the reaction chamber by spraying ammonium sulfate solutions in two steps with concentrations of 4g/L and 40 g/L. The particles were dried by passage through a silica gel diffusion tube and size selected at an electromobility diameter d = 100 nm. Increasing amounts of ammonium sulfate seed particles instantaneously led to lowered HOM concentrations in the gas phase due to the additional loss by condensation on the seed particles. The decrease in signal intensity with increasing particle surface was used to evaluate γ_{eff} as described below.

We operate our chamber as a continuously stirred tank reactor (CSTR) in a flow through mode with a well-mixed core of the chamber. HOM lost at the chamber walls must diffuse through the laminar boundary layer at the chamber walls. In the chamber with no aerosols present, the walls constitute the major sink of HOM. In this case the observed steady state concentration is determined to a very good approximation only by the production rate and the wall loss rate. When seed aerosol is added or new particles are formed, the additional condensational sink provided by the particle surface lowers the steady state concentration. Under conditions of unperturbed gas-phase production and typical times for phase transfer smaller than the residence time of the air in the chamber, the lowered gas-phase steady state concentrations reflect the partitioning of HOM, which is determined by the balance of condensation and evaporation. (Tröstl et al. (2016) noted that HOM can be LVOC i.e. they have a very small but noticeable vapor pressure.) Since we are working in a steady state system, we cannot easily separate between a kinetically slow uptake and a balance between (fast) uptake in steady state with a (fast) evaporation.

For molecules with noticeable volatility steady state between condensation and evaporation is established on the time scales of less 10 minutes in our CSTR, e.g. for molecules with molecular masses of 300 Da and at a particle surface of 5.0×10^{-4} m^2 m^{-3} the typical uptake time is about the same as the mixing time of 120 s. We express the net effect of condensation and evaporation by an effective uptake coefficient γ_{eff} and the gas kinetic collision rate of HOM with the particle surface. The γ_{eff} can be determined by measurement of the ratio of steady state HOM concentrations for the unseeded case and for seeded cases with the advantage that only signal intensities are required and hence no calibration is needed (Sarrafzadeh et al., 2016).

Size selection by electromobility produced bimodal size distributions in the chamber over the times of observation of 2 h and 3.5h with one mode around 100 nm and a second mode around 200 nm (≈25% by number). The diameter of the median of the surface distributions was located in a range of 150 - 200 nm. Since it is likely that nearly every collision with the surface of particles will lead to phase transfer of HOM, we considered the Fuchs-Sutugin correction factor (f_{FS}) to calculate the collision rate (Fuchs and Sutugin, 1971) in order to correct for diffusion limitations. Taking into account the mean free path for a range of molecular compositions of $C_{10}H_{14\text{-}16}O_{4\text{-}12}$ and a median of the particle surface distribution in a range of 150-200 nm, we estimate f_{FS} in a range of 0.65-0.75; diffusivity was calculated after Fuller et al. (1969).

In a first step wall loss rates of HOM were measured. After stopping the OH production and thus photochemical HOM formation we observe an exponential decay of HOM signals. The exponential decay of the signal intensity gives the lifetimes of those HOM. In absence of particles the lifetimes reflect the wall loss rates. As shown in Sarrafzadeh et al. (2016) and Ehn et al. (2014) the lifetimes were in the range of 70 to 150 s, i.e. the loss rates on the walls of the chamber, L_W(HOM), were in the range of 1.4×10^{-3} to 7×10^{-3} s^{-1}. L_W(HOM) are more than order of magnitude higher than those caused by the flush out of the air in the chamber (3.6×10^{-4} s^{-1} for the residence time of 46 minutes). Therefore we neglected flush out as sink for HOM. In a second step, the chemical system was kept at the same steady state conditions for $[OH]_{SS}$, $[O_3]_{SS}$, and MT concentration. Data evaluation was based on the following considerations: The concentration of any HOM, c(HOM) is determined by its production rate P(HOM) and the first order loss rate, L(HOM) as given in Eq. (4):

$$c(HOM) = \frac{P(HOM)}{L(HOM)} \quad (4)$$

In absence of particles the total loss rate L(HOM) is given alone by the loss rate at the chamber walls, L_W(HOM). In presence of particles L(HOM) is the sum of loss rates at the walls and at the particle surface, L_W(HOM) + L_p(HOM). At constant production rate P(HOM) the ratio of concentrations is inverse proportional to their ratio of loss rates:

$$\frac{c(HOM)^0}{c(HOM)} = \frac{L_W(HOM)+L_P(HOM)}{L_W(HOM)} \quad (5)$$

In Eq. (5), $c(HOM)^0$ is the concentration of HOM in the particle free chamber and c(HOM) is the concentration in the particle containing chamber. Solving Eq. (5) for L_p(HOM) we achieve Eq. (6):

$$L_P(HOM) = \frac{c(HOM)^0}{c(HOM)} \cdot L_W(HOM) - L_W(HOM) \quad (6)$$

We varied the surface area of seed particles (S_P) and determined L_P(HOM) by Eq.(6). We found a linear relationship between L_P(HOM) and S_P as expected from kinetic gas theory, Eq. (7):

$$L_P(HOM) = \gamma_{eff} \cdot f_{FS} \cdot \frac{\bar{\upsilon}}{4} \cdot S_P \quad (7)$$

In Eq. (7), f_{FS} is the Fuchs-Sutugin correction, $\bar{\upsilon}$ is the mean molecular velocity of the HOM, and γ_{eff} is an effective uptake coefficient. The coefficient γ_{eff} was obtained from the slope of such plots by dividing the values for slopes by $f_{FS}\times\bar{\upsilon}/4$ with f_{FS} = 0.7 assuming a mean median of the surface size distribution of 175 nm. In case of β-pinene some new particle

formation was observed which hindered measuring $c(HOM)^0$ directly. Here, $c(HOM)^0$ was calculated by linear extrapolation of $1/c(HOM)$ to zero particle surface (compare to supplement, Section S3).

It has to be noted that γ_{eff} is only valid, if S_P is not too large for two reasons. First, in presence of a strong condensational sink, many HOM signals become close to the detection limit (here for S_p >1.2×10^{-3} m^2 m^{-3}). Secondly, for large S_p (>2×10^{-3} m^2 m^{-3}) distinct deviations from linearity were observed, likely due to fact that the time scales of losses of peroxy radicals on particles become similar to the time scales of peroxy radical reactions (Pullinen, 2017). If so, the production rates P(HOM) of HOM termination products are not constant but decrease significantly with increasing particle load.

3 Results

3.1 Yields of organic nitrates from β-pinene photo-oxidation

In the first step we determined the potential of organic nitrate (ON) formation in a β-pinene / NO_X mixture ([β-pinene]$_0$ ~39 ppb / [NO_X]$_0$ ~50 ppb). The β-pinene and NO_X were added to the chamber that contained about 60 ppb O_3. The OH production was started by switching on the UV lamp (time = -2.4h in Figure 1), inducing the photochemical oxidation of β-pinene and thereby the ON production. As shown in Figure 1, concentrations of *β*-pinene and NO_X decreased in the presence of OH. When the photochemical system was in a steady state after about two hours (time t = 0 h in Figure 1) the *β*-pinene addition was stopped and *β*-pinene concentration decreased to zero. In parallel, [OH] increased leading to a lower NO_X concentration. At time t = 1.7 h, the OH concentration was re-adjusted to the same OH level as before the removal of *β*-pinene by lowering J(O^1D). The decrease in [OH] caused an increase of [NO_X] by 15 ppb to 32 ppb. Considering the NO_X level of 20 ppb before the *β*-pinene had been removed, the net NO_X increase amounts to 12 ppb. The inflow of NO_X as well as the OH concentration were the same before and after removal of *β*-pinene, but now [NO_X]$_{SS}$ was higher. Hence, with *β*-pinene we removed a strong NO_X sink in the chamber. Most of this NO_X sink is made up by reactions of NO and NO_2 with peroxy radicals and peroxy acyl radicals that lead to ON formation (reactions R6a and R7). Thus, the difference in [NO_X]$_{SS}$ in presence and in absence of *β*-pinene allowed to calculate the fraction of ON formed from β-pinene. Defining the yield of ON formation as the molar amount of NO_X "released" by not forming *β*-pinene ON over the molar amount of consumed *β*-pinene and with the assumption that one lost NO_X molecule had produced one ON molecule we derived a molar yield of ~36% for the ON formed from *β*-pinene. For later comparison with AMS results we calculated the mass concentration of nitrate bound to the organic moieties ($OrgNO_3$), again with the assumption that one lost NO_X molecule produces one $OrgNO_3$. A total mass concentration of 33 µg m^{-3} $OrgNO_3$ in the gas phase was obtained at the given condition in the chamber. The mass concentration of HNO_3 formed during this time was about 24 µg m^{-3} (for details of these calculations see supplement section S3).

3.2 HOM formation from α-pinene- and β-pinene photo-oxidation

We observed multifunctional peroxy radicals (HOM-RO_2) as well as their termination products in the high resolution mass spectra. The latter are formed in accordance with established pathways of peroxy radical chemistry (Bianchi et al., 2019). We will distinguish HOM-PP, which arise from permutation reactions of HOM-RO_2 with peroxy radicals including HO_2, and HOM-ON, which are formed in reaction of HOM peroxy and HOM acyl peroxy radicals with NO or NO_2. In addition we found HOM accretion product with $C_{>10}$ and $C_{<20}$ (HOM-ACC).

We observed two major differences in HOM formation and product patterns for α-pinene and β-pinene, which are both related to the position of their double bond:

1. For α-pinene, with an endocyclic double bond, addition of ozone is relatively fast and at OH concentrations up to $1x10^7$ cm^{-3} certain fractions of HOM were produced by ozonolysis (compare supplement Figure S6). In contrast, ozonolysis of β-pinene, with an exocyclic bond, is slow and does not produce significant amounts of HOM (Pullinen, 2017).
2. The HOM products of α-pinene in the monomer region mainly consisted of C_{10}-molecules, as breaking of an endocyclic double bound will merely lead to ring opening. The breakage of the exocyclic double bond of β-pinene during the oxidation process will cause some fragmentation. We observed progressions of C_{10}, C_9, C_8, and C_7 HOM leading to overlapping peaks in the mass spectra. E.g. molecular masses where 1 C-atom and 4 H-atoms are replaced by 1 O-atom were not fully resolved. However, by peak fitting we were able to attribute the contributing formula components in most cases (see supplement section S2 and peak list in supplement section S6). In addition, fragmented peroxy radicals in β-pinene form a larger variety of accretion products with less than 20 C-atoms.

Besides these differences, the behavior with respect to NO_X addition was very similar for α-pinene and β-pinene photo-oxidation: increase of HOM-ON (increase of peaks with odd molecular masses odd peaks), decrease of accretion products and a shift of HOM monomers to the higher *m/z*.

3.3 Accretion products and products from fragmentation

With increasing NO_X we observed a strong decrease of HOM-ACC relative to HOM monomers. These can be clearly seen in the HOM mass spectra obtained for α-pinene and β-pinene in Figure 2 by comparing the ranges of $m/z < 340$ Da and $m/z > 420$ Da for low and high NO_X conditions. To quantify the effect, the molecular mass weighted signals of HOM-monomers (C_5-C_{10}, 230 Da < m/z < 550 Da) and HOM-ACC products (C_{11}-C_{20}, 230 Da < m/z < 550 Da were converted to mass concentrations, summed up and normalized as described in supplement section S3. Figure 3 shows the mass concentration of total HOM and the fractions of HOM monomers and HOM-ACC as function of NO_X. HOM-ACC decrease with NO_X: at low NO_X conditions, accretion products contributed ≈40 % and monomers contributed ≈60 % to the total mass concentration of

HOM. At the highest NO_X level the mass concentration of HOM-ACC was suppressed by about 70%. In comparison, the sum of HOM monomers was diminished only by less than 10 %. The decrease of HOM-ACC mixing ratio is attributed to the competition between HOM-ON formation channels (R6a and R7) and HOM-ACC formation channel (R5). As we will show in the next section, in presence of NO_X more HOM-ON monomers were formed and thus less HOM accretion products.

We separated HOM monomers in compounds with C_{10} and compounds with $C_{<10}$ (C_{5-9}). As shown in Figure 3 the mass concentration of $C_{<10}$ HOM increased with $[NO_X]_{SS}$ whereas C_{10} HOM decreased. This indicated that a portion of $C_{<10}$ arose from fragmentation of alkoxy radicals formed in R6b. However, since we consider only molecular masses ≥ 230 Da, which is the molecular mass for formula $C_{10}H_{14}O_6$, the $C_{<10}$ compounds must still be highly functionalized, i.e. they must carry more oxygen than the respective C_{10} compounds to reach similar molecular masses, actually one O atom more per C lost.

Since total HOM decrease at higher $[NO_X]_{SS}$, but HOM monomers remain about stable over the whole NO_X range, the suppression of the HOM-ACC were the cause for the reduction of total HOM and therewith of condensable mass. The fragmentation via alkoxy radicals played only a minor role.

3.4 Detection of termination permutation products of peroxy radical - peroxy radical reactions and HOM-organic nitrates

At low NO_X conditions, HOM-PP with even molecular masses showed the highest concentrations. HOM-ACC are also produced from peroxy-peroxy permutation reactions, but their intensity decreased strongly and HOM-ACC are barely observed at high NO_X condition, as described in previous section 3.3. For that reason, we focus on monomer products in the following considerations in section 3.5-3.7.

Because of the complexity of the product spectrum the character of the functional group formed in the termination step of HOM-PP cannot be derived unambiguously from the available elementary molecular formulas alone. As an example, HOM-PP with the molecular formula $C_{10}H_{16}O_X$ can be hydroperoxides formed from peroxy radicals with molecular formula $C_{10}H_{15}O_X$ in reaction R3a, they can be alcohols formed from peroxy radicals $C_{10}H_{15}O_{X+1}$ in reaction R4a, or they can be ketones formed from peroxy radicals with the molecular formula $C_{10}H_{17}O_{X+1}$ in reaction R4a. Dependent on the specific precursor peroxy radical, they can also be carboxylic acids or percarboxylic acids. We therefore lump the monomer HOM with even masses (HOM-PP) together independent of the chemical character of the termination group. In case of β-pinene, we did not separate the contributions from different progressions (e.g. $C_{10}H_YO_X$ and $C_9H_{Y-4}O_{X+1}$) but used the overall signal under the peak for further analysis and indicate the main components under the peak (e.g. Figure. 5). Separation between HOM-PP and HOM-ON was easier, because HOM-ON have odd molecular masses. Peroxy radicals (without N) also contribute to the odd mass peaks, but in most cases they could be separated by the mass defect. Other contributors to odd mass peaks are HOM containing ^{13}C and clusters with the nitrate dimer ($HNO_3NO_3^-$) of HOM-PP, but the latter contribution was small (supplement section S2). Analysis of the high resolution mass spectra for *α*-pinene revealed that HOM-ON-peroxy radicals are rare. Peak lists for the HOM measured in the absence and presence of NO_X are given in the supplement section S6. (Note that we cannot *a priori* distinguish between HOM-ON formed in reactions R6a and R7, respectively).

Figure 4 demonstrates the change in the HOM pattern when NO_X is added to the reaction system. At low NO_X levels, HOM-PP (black) were predominant, but already at the medium NO_X levels the concentrations of HOM-ON (blue) were similar to HOM-PP (black). HOM-ON concentrations increased on the cost of HOM-PP. The product spectra of β-pinene showed a similar shift from HOM-PP to HOM-ON.

With increasing NO_X we observed a small but increasing fraction of highly oxidized nitrates with C<10. Their chemical formulas have low H:C ratio compared to gas-phase C_{10} HOM-ON. Supposedly, they did not arise from gas-phase chemistry but were likely formed at the walls. Their time series was not responding to the changes of experimental conditions like start of photochemistry or cease of NO_X addition, instead these compounds increased steadily after NO_X addition. For α-pinene, their maximum contribution appeared at 74 ppb $[NO_X]_{SS}$ where they mounted up to 8% of the total HOM concentration and 17% of the HOM-ON concentration. Below 35 ppb NO_X their contribution was less than 7% and 12%, respectively. For β-pinene, this was less distinct and the contribution was only 2 to 3 %. Because these HOM-ON had C<10 and appear at the lower end of the mass spectrum, their contribution to HOM mass (and therewith SOA mass) were small, and we did not correct for these products.

3.5 Effective uptake coefficients for HOM-PP and HOM-ON.

Based on identified HOM-ON and HOM-PP, we characterized their potential contribution to SOA formation by determining their loss rates on seed particles L_P(HOM), Eq.6. According to Eq.7, plots of L_P(HOM) versus particle surface, S_P, should exhibit a linear dependence between L_P(HOM) and S_P allowing for determining effective uptake coefficients, γ_{eff}. However, for conditions with sufficient HOM production, we could not fully suppress new particle formation in absence of seed particles. As a result $c(HOM)^0$ in Eq.5 and 6 had to be determined by extrapolating 1/c(HOM) as f(S_P) to S_P=0. The wall loss coefficient L_W(HOM) was determined to 150s in independent experiments at lower concentrations and in absence of new particle formation. With $c(HOM)^0$ and L_W(HOM) L_P(HOM) was calculated allowing to derive γ_{eff} from Eq. (7) by applying f_{FS} = 0.7 to the slope of L_P(HOM) as a function particle surface S_P (Figure 5). Figure 5 is based on HR data, which show substantial scatter. The UMR data showed a better signal to noise ratio than the individual HR peaks under the same UMR signal. In order to reduce the scatter we thus used the respective unit mass resolution (UMR) data for the evaluation of γ_{eff}. In Figure 6 we compare γ_{eff} for HOM with the same number of O-atoms. Note that compared to their chemical sum formula, ON were shifted by one O to lower O in order to account for the addition of NO. When comparing data for HOM with the same numbers of O-atoms (in the precursor peroxy moiety), no significant and systematic differences were found for γ_{eff} within the uncertainty limits, i.e. the potential to condense on particles was about the same for HOM-PP and HOM-ON. For HOM moieties with 8 and more O-atoms, γ_{eff} approaches 1 independent if they were HOM-PP or HOM-ON. HOM-PP and HOM-ON with 6 and more O-atoms with upper limits of γ_{eff} near 0.5 will still reside to a large portion in the particle phase therefore they should also contribute significantly to SOA mass.

3.6 Organic bound nitrate in SOA and in gas-phase HOM-ON

SOA yields for α-pinene and β-pinene (wall loss corrected) were between 0.08 and 0.18, thus in the same range as those reported by Sarrafzadeh et al. (2016). The amount of formed SOA mass and the SOA yields changed with addition of NO_X to the photochemical system because NO_X affects $[OH]_{SS}$ and thereby also the formation of higher generation products. The mass fractions of $OrgNO_3$ in the SOA particles are shown in Figure 7. They were calculated for the different NO_X concentrations by dividing the mass concentration of $OrgNO_3$ by the mass concentration of the respective organic as measured with the AMS. The fraction of $OrgNO_3$ in particles was dependent on the NO_X concentrations. It was negligible when no NO_X was added and increased steadily with increasing $[NO_X]$. At the same time, also the fraction of inorganic nitrate increased with increasing $[NO_X]$, but was a factor of about 3 lower than that of $OrgNO_3$ (Figure 7). Calculating $[HNO_3]_{SS}$ in the gas phase from $[NO_2]$ and [OH] shows that, at highest NOx concentrations up to 24 µg m^{-3} HNO_3 were formed in the gas phase, but less than 0.1 µg m^{-3} of inorganic nitrate was found in the particle phase. For the same $[NO_X]_{SS}$, the mass fractions of organic or inorganic nitrate in SOA were about the same for α-pinene and β-pinene, indicating that the formation of condensable $OrgNO_3$ was similar. The determination of $OrgNO_3$ comprises some uncertainty, but even if we count all inorganic nitrate as $OrgNO_3$ we get an upper limit of less than 4%.

We compared the amount of $OrgNO_3$ in particles to that in the gas phase. As shown in section 3.1, at $[NO_X]_{SS}$ ~20 ppb about 33 µg m^{-3} $OrgNO_3$ was formed in the gas phase. At similar $[NO_X]_{SS}$ and similar β-pinene concentrations ($[NO_X]_{SS}$ ~22 ppb, $[\beta\text{-pinene}]_{SS}$ ~6 ppb) the fraction of $OrgNO_3$ in the particle phase was only 1.6 ± 0.64 % (Fig. 7), i.e. less than 0.4 µg m^{-3} $OrgNO_3$ was bound in particles. We conclude that many ON are too volatile to significantly contribute to the particulate phase. However, considering the low volatility HOM-ON (section 3.5), HON-ON should contribute to particle mass eventually providing the particulate $OrgNO_3$. We estimated the mass fraction of $OrgNO_3$ bound in HOM-ON. For this we considered all HOM with 6 and more O-atoms in the HOM-moiety (molecular mass >230 Da) because their γ_{eff} is large enough to partition significantly into the particle phase and to contribute efficiently to SOA mass. As shown in Figure 6, the HOM partitioned without preference, independent of being HOM-PP or HOM-ON. We first determined the fraction on a molecular base by using the ratios of signal intensities, which is identical to using concentrations c:

$$\frac{c(HOM-ON)}{c(all\ HOM)} \approx \frac{\sum_{241}^{405} c(HOM-ON)}{\sum_{230}^{550} c(allHOM)} \qquad (8)$$

In Eq.8, the left hand term represents the molar fraction of HOM-ON. We summed all HOM with O ≥ 6, which included all HOM with γ_{eff} >0.5 and provides a lower limit. Signals at m/z>550 Da were not taken into account, since they were very low at high NO_X levels and thus uncertain. In a second step we calculated from Eq.8 the mass ratio of $OrgNO_3$. We split all HOM in the denominator of Eq.8 in HOM-ON and other termination products and multiplied the concentrations with the respective molar weight (Eq.9). The enumerator was multiplied with the molecular weight of the nitrate termination group:

$$\frac{M(OrgNO_3)}{M(organic)} \approx \frac{\sum_{241}^{405} c(HOM-ON)\cdot 62}{\sum_{230}^{550} c(other\ term.prod.)\cdot m + \sum_{241}^{405} c((HOM-ON)\cdot(m-62))} \quad (9)$$

In words, the left hand term in in Eq.9 gives the ratio of the total mass of $OrgNO_3$ over the total organic mass of HOM with $\gamma_{eff} > 0.5$ ($O \geq 6$). This value can be compared with the direct AMS observation of $OrgNO_3$. Figure 8 shows the molecular ratios (calculated by Eq.8) and the mass fractions (Eq.9) in dependence on NO_X. For α-pinene we were able to separate HOM-ON and HOM-RO_2 unambiguously (see supplement). For β-pinene we give lower and upper limits of the molecular and mass fractions, because of uncertainties in the HR analysis that were induced by the stronger fragmentation and overlapping progressions of compounds with different number of C but same unit molecular mass. For the lower limit shown in Figure 8, we applied a peak list with all identified signals at low and high NO_X concentrations for fitting, whereas the upper limit was achieved by using the peak list optimized for high NO_X cases. (The reason for the spread can be explained as follows: the approach with the peak list with all identified peaks attributes some HOM-RO_2 to the HON-ON signal, independent if the specific HOM-RO_2 exist in the chemical system or not, while the approach with the high NO_X peak list has the tendency to falsely attribute HOM-ON to existing HOM-RO_2 missing in the high NO_X peak list.)

Both, HOM-ON and $OrgNO_3$ mass fraction increased with $[NO_X]$, similarly for both MT. For α-pinene about 40 % of the detected HOM were HOM-ON and more than 10 % of the HOM mass was $OrgNO_3$ once $[NO_X]$ was larger than 30 ppb ($[BVOC]_{SS}/[NO_X]_{SS}$ < 2 ppbC/ppb). For upper limit case of β-pinene we achieved about the same fractions as observed for α-pinene (50 ppb NO_X : $[BVOC]_{SS}/[NO_X]_{SS}$ < 1.1 ppbC/ppb). Since we considered only HOM that efficiently condense on particles, one would expect that $OrgNO_3$ brought by HOM-ON alone should contribute about 10 % of the SOA mass. This was not the case, as the direct comparison in Figure 8 shows. The maximum contribution of particulate $OrgNO_3$ was about 3 %, i.e. the measured $OrgNO_3$ was a factor of 3 to 4 lower than expected: the $OrgNO_3$ bound in low volatility HOM-ON which could potentially contribute to SOA mass was significantly higher than $OrgNO_3$ directly observed in the particle phase.

3.7 Mass concentration of HOM

To estimate an possible effect of hydrolysis of $OrgNO_3$ and re-evaporation of HNO_3, potential condensable mass concentration (c^{Mass}) was derived by weighing the concentration (c_i^N) of each HOM_i by its molecular mass (M_i) in the range of 230 Da to 550 Da:

$$c^{mass} = \sum_{230}^{550} c_i^N \cdot M_i$$

Herein c^N is the concentration that was corrected according to the method described in supplement section S2. Figure 9 shows the calculated mass concentrations with and without hydrolysis in dependence on NO_X. The relative uncertainty limits were estimated to 19%. The uncertainty was estimated from the standard deviation of the data obtained at low $[NO_X]$ conditions (9 measurements). Uncertainties of $[NO_X]_{SS}$ were estimated to be ± 10%. The uncertainty of absolute concentrations caused by the uncertainty of the calibration factor (see supplement S1) is much higher than the uncertainty limits shown in the Figure 9. However, as the systematic error of the calibration factor is the same for each data point it does not affect the observed trend of only somewhat decreasing mass concentrations of HOM with increasing NO_X.

In case of HOM-ON, c^{mass} includes the mass of $OrgNO_3$. According to many studies particulate ON is undergoing hydrolysis, leading to loss of HNO_3 (Bean and Hildebrandt Ruiz, 2016; Boyd et al., 2015; Rindelaub et al. 2015; Takeuchi and Ng, 2017). It is not clear if organic material lost from the particulate phase besides $OrgNO_3$ (Fisher et al., 2016, Takeuchi and Ng, 2017, Zare et al. 2019). The efficiency of the hydrolysis of $OrgNO_3$ depends on RH and particle acidity and several studies report fractions of hydrolyzed particulate ON in a range of 10 - 60% (Bean and Hildebrandt Ruiz, 2016; Boyd et al., 2015; Browne et al., 2013; Rindelaub et al. 2015; Takeuchi and Ng, 2017).

We indicate the resulting SOA mass after considering $OrgNO_3$ loss by hydrolysis and evaporation of HNO_3 by a prime as cmass' in Figure 9 (details for the calculations of cmass' see section 4.3). It is obvious from Figure 9 that the mass concentration of condensable HOM is about 30% lower at the highest NO_X conditions compared to those at low NO_X conditions. It is furthermore evident that the differences between c^{mass} and $c^{mass'}$ are quite low which is showing re-evaporation of HNO_3 is of minor importance for explaining the SOA mass suppression with increasing NO_X in the system. An explanation must then be the observed strong decrease of the accretion products with increasing NO_X as shown in Figure 2.

4 Discussion

4.1 Organic nitrates and SOA formation.

Several studies on organic nitrates (ON) or organic bound nitrate ($OrgNO_3$) in SOA refer to reactions of unsaturated volatile organic compounds with NO_3 (Claflin and Ziemann, 2018; Faxon et al., 2018; Fry et al., 2013, 2014; Kiendler-Scharr et al., 2016; Lee et al., 2016a, Ng et al., 2017 and references therein). The pathway of forming ON by NO_3 was negligible in our experiments as we applied quite high light intensity, humidity and also high NO concentrations during our experiments. These experimental conditions inhibited formation of NO_3 at relevant concentrations because NO_3 was efficiently destroyed by photolysis, by reactions with NO and by scavenging of N_2O_5 at the humid surfaces of the chamber walls. The HOM-ON measured during our experiments were formed in reactions R6a and R7.

There are some studies with respect to the SOA content of ON formed by photo-oxidation (Berkemeier et al., 2016; Lee et al., 2016b; Nozière et al., 1999; Rollins et al., 2010; Takeuchi et al., 2019; Xu et al., 2015b; Zhao et al., 2018) wherein in most cases mass fraction of ON of the total SOA mass is reported. According to literature data, ON produced during photo-

oxidation or ozonolysis contribute between 3 % (Lee et al., 2016b) and 40% (Berkemeier et al., 2016) to the total SOA mass. This compares well with the mass fraction of HOM-ON with molecular masses >230 Da, which varied from 0-50% with increasing NO_X (Figure 4). HOM-ON (>230 Da) provide a measure of the expected contribution of ON to SOA as HOM-ON and all other HOM should condense with same efficiency as shown by their γ_{eff} in Figure 6.

We determined $OrgNO_3$ by the AMS as a diagnostics for ON in the particulate phase. The $OrgNO_3$ mass fractions ranged from 0 % (no NO_X addition) to 2.7 %, which is within the range 0.6 - 8% of most literature data but at the lower end (Nozière et al., 1999; Rollins et al., 2010; Xu et al., 2015b; Berkemeier et al., 2016; Lee et al., 2016b; Zhao et al., 2018). (When mass fractions of particulate ON were given, we estimated $OrgNO_3$ assuming an average molecular mass of 300 Da and one nitrate group per ON; see supplement section S5). In our study we showed that $OrgNO_3$ depends on the NO_X level ($[VOC]/[NO_X]$ level) as expected from established peroxy radical chemistry in presence of NO_X. This finding can probably explain the wide range of ON and $OrgNO_3$ fractions reported for SOA formation in presence of NO_X. Detailed and meaningful comparison of our data to those reported in literature requires knowing the $[VOC]/[NO_X]$ ratios during SOA formation in the respective experiments. The $[VOC]/[NO_X]$ ratio is known for experiments made by us in the SAPHIR chamber in Jülich (Zhao et al., 2018). Zhao et al. (2018) achieved a mass fraction of 11% for $OrgNO_3$ which is significantly higher than the $OrgNO_3$ mass fractions in this study. Interestingly, the 11% found by Zhao et al. (2018) are close to the 10% mass fraction of $OrgNO_3$ determined for the total HOM in this study. These findings will be further discussed in section 4.3.

4.2 Effective uptake coefficients

We provided data on effective uptake coefficients, γ_{eff} , which allowed differentiation between SVOC, LVOC and ELVOC. The dependence of γ_{eff} on the number of O-atoms in the HOM (Figure 6) suggests that the $OrgNO_3$ found in SOA predominantly originates from HOM-ON with 6 and more O-atoms (without -NO). We conclude that ON with less than 5 O-atoms are not so important for the formation of SOA at least at small loads of SOA. This conclusion is confirmed by our observation of small mass fractions of $OrgNO_3$ in HOM monomers (0-10%) and in the particle phase (0-3%) despite of the large ON fractions produced overall in the gas phase (molecular yield > 30%, Figure 1 in section 3.1) . From all ON only a few percent - the HOM-ON - made it into the particulate phase (sections 3.1 and 3.6).

Our findings are in agreement with observations by Lee et al. (2016b) in a field study. They also show that the distribution of signal intensities for HOM-ON in the gas phase is different from that in the particle phase. Comparing the signal intensities for HOM-ON with the same number of O-atoms between gas phase and particle phase, respectively (Figure 2 in Lee et al., 2016b), it seems that the higher the number of O-atoms, the more the ON partition in the particle phase. As there was no calibration for gas phase HOM-ON, absolute numbers for partitioning coefficients or effective uptake coefficients were not obtained. Our data are qualitatively consistent with those of Lee et al. (2016b), suggesting that the basics of HOM-ON condensation in our laboratory studies are similar to those in the environment.

Comparison between γ_{eff} determined for HOM-PP and HOM-ON indicated that there were no significant and systematic differences at least for the HOM moieties with more than 6 O-atoms. The variability in γ_{eff} in Figure 6 is probably caused by the fact that more than one compound with different structure and functionalization is contributing to each data point. E.g. $C_{10}H_{16}O_x$ showed a large γ_{eff} at O number of 7 (Figure 6). The signal assigned to $C_{10}H_{16}O_7$ could be dominated by a compound with extreme low vapor pressure.

The independence of the overall uptake behavior from the termination groups can be understood from the basics of group contribution models (Capouet and Müller, 2006; Pankow and Asher, 2008): HOM peroxy radicals with more than 6 O-atoms already carry protic functional groups - OH, -OOH, C(=O)OH, or C(=O)OOH - from the several autoxidation steps. Thus their vapor pressure is low because of the ability to form (multiple) hydrogen bonds. The termination reactions R3, R4a, R6a, and R7 only form one more functional group of the respective HOM. Except of the functional group added by the termination reaction, distributions of functional groups are the same for all monomer termination products originating from the same HOM peroxy radical. This also includes HOM-ON. Hence, no substantial differences should be expected for the vapor pressures of all monomer termination products produced originating from the same HOM peroxy radical.

Considering the molecular mass instead of O-atoms of the HOM moiety, HOM-ON have higher vapor pressure compared to HOM-PP (Peräkylä et al., 2019), despite of the heavier termination group -ONO_2 compared to -OOH, =O, or -OH. Note, that the number of functional groups cannot be inferred one to one from the number of O-atoms. HOM-peroxy radicals can be formed via autoxidation of peroxy radicals or via H-shifts and O_2 addition in alkoxy radicals and thus there may be different numbers of O-atoms per functional groups. In addition, peroxy radicals may have the same molar weights but may have different molecular structures. With this limitation in mind, we will exploit the relationship between γ_{eff} and O atoms as proxy for the number of functional groups in the next step of interpretation.

Starting from a given HOM-peroxy radical, the number of functional groups in the termination products is the same, independent if a HOM-PP or a HOM-ON is being formed. However, the masses of HOM-PP and HOM-ON differ. If a HOM-ON is formed, it contains 1 N and 1 or 2 O-atoms more than the parent HOM peroxy radical (depending on NO or NO_2 being added). If a HOM-PP is formed in a reaction of the same HOM peroxy radical with another peroxy radical, HO_2 or RO_2, the number of O-atoms stays constant in case of hydroperoxide formation or decreases by 1 in case of ketone or alcohol formation. This means that the formation of HOM-ON generally increases the molecular mass compared to a HOM-PP (as was considered in Figure 6). Since the γ_{eff} are similar for all monomer HOM originating from the same HOM peroxy radical, i.e. HOM-PP and HOM-ON have similar vapor pressures, a gain of SOA mass could be expected if HOM-ON are produced instead of HOM-PP (≈10% gain per HOM-ON for NO and at a molecular mass of 300 Da). However, whether this potential mass gain can be realized at all in a long term net increase of SOA mass in NO_X containing systems will depend on the fate of the ON in the particle phase.

4.3 Comparison of $OrgNO_3$ in HOM to $OrgNO_3$ in particles

Comparing the data shown in Figure 8, it is obvious that the mass fraction of $OrgNO_3$ in gas-phase HOM is 3 to 4 times higher than that found in the particulate phase. As all considered HOM (molecular mass > 230 Da) have a high efficiency for SOA formation, a fraction of about 10 % $OrgNO_3$ would be expected in the particle phase. Zhao et al. (2018) performed experiments of α-pinene photo-oxidation in presence of 20 ppb NO_X at a lower relative humidity of ≈30% in the SAPHIR chamber in Jülich. Of course there are differences between steady state experiments in JPAC and time dependent experiments in the batch reactor SAPHIR; However, applying the same instrumentation and using the same evaluation schemes as here, Zhao et al. (2018) find a mass fraction of 11% for $OrgNO_3$ in the particulate phase, i.e. mass closure as expected if all HOM with more than 6 O-atoms contribute to SOA formation. This is more than the 2-3% $OrgNO_3$ that we realized in the particulate phase. A difference between the experiments here in JPAC and Zhao et al. (2018) in SAPHIR was the relative humidity which was about 30 % by Zhao et al. (2018) and 63% in the study here. We suggest that the RH may be the key to bring this study and the results by Zhao et al. (2018) in agreement, although we cannot provide further experimental proof. However, there are several studies implying that ON undergo hydrolysis in the condensed phase (Bean and Hildebrandt Ruiz, 2016; Boyd et al., 2015; Browne et al., 2013; Day et al., 2010; Fisher et al., 2016; Jacobs et al., 2014; Lee et al., 2016b; Liu et al., 2012; Rindelaub et al., 2016, 2015). Thus, hydrolysis can be suspected as a mechanism explaining both, the lower fraction of $OrgNO_3$ in the particle phase compared to that stored in HOM organic nitrates and the lower amount or $OrgNO_3$ found in this study compared to that found by Zhao et al. (2018).

In addition, hydrolysis of $OrgNO_3$ could contribute to SOA mass suppression. We estimated the effect of ON hydrolysis on the remaining SOA mass under the assumption that all HOM-ON with $\gamma_{eff} > 0.5$ had condensed on SOA. By hydrolysis of organic nitrates HNO_3 is formed and the nitrate functionality at the organic rest is replaced by an OH group (Hu et al., 2011). HNO_3 is too volatile to stay in the particle phase (e.g., Browne et al., 2013; Romer et al., 2016) and we found only negligibly small amounts of inorganic nitrate in particles despite of high HNO_3 production in the gas phase (section 3.1). As a consequence, on average 1/5 of the mass of the HOM-ON that originally condensed on particles might re-evaporate and indeed reduce the amount of condensed mass. The question is what happens to the remaining organic moiety. As long as hydrolysis does not lead to fragmentation of the organic rest, hydrolysis just replaces the nitrate group by the protic OH group. The number of functional groups remains the same and no strong changes in the vapor pressures are expected for the organic rest. As a consequence the organic rest of the former organic nitrate would stay in the particle phase. If so, hydrolysis and re-evaporation of HNO_3 should not lead to a mass loss high enough to explain the often observed suppressing effect of NO_X on SOA mass formation in laboratory studies. The mass loss per evaporated HNO_3 is 63 Da. The water molecule driving the hydrolysis can be from gas-phase or particulate phase and exchange of water between the phases is fast. The de facto mass loss therefore should be 45 Da per evaporating HNO_3. A part of this loss is "compensated"; depending on the HOM-ON being formed by NO or NO_2 and, depending on the HOM-PP not produced instead of the organic nitrate, this mass gain is between 29 Da and 63 Da per formed HOM-ON. Thus, the net effect of mass gain by the formation of a HOM-

ON instead of a HOM-PP in the gas phase and the possible mass loss due to evaporation of HNO_3 from the particle phase should be very low or negligible.

4.4 Suppression of accretion products and SOA yield

In the previous section we have shown that the formation of organic nitrates instead of other HOM monomer termination products cannot explain the suppressing effect of NO_X even if we consider hydrolysis and loss of HNO_3. Also increasing fragmentation via alkoxy radicals from reaction R6b seemed to play only a minor role (see section 3.3, Figure 3). Reasons are that fragments formed in α-scission can still be highly functionalized, thus are simply HOM with less C atoms. In addition bond scission in alkoxy radicals of α- and β-pinene can lead to ring opening retaining the carbon number. Moreover, isomerization of alkoxy radicals is another pathway (unimolecular or bimolecular) that leads eventually to peroxy radicals with same number of carbon atoms that could undergo further autoxidation and/or terminate to highly functionalized HOM (Vereecken et al. 2009, 2010).

The most probable explanation for the NO_X induced suppression of SOA formation in laboratory studies is the suppression of HOM-ACC formation. At low NO_X conditions, the mass fraction of HOM-ACC is similar to those of monomers and it dropped to less than 30% at high NO_X (Figure 3). Hence, besides reduction of [OH] at high NO_X, suppression of HOM-ACC formation by NO_X might lead to a strong suppression of SOA formation in laboratory studies.

The precursors of the respective HOM-ACC are the key to understand how the suppression of HOM-ACC formation could lead to a suppression of SOA formation. As we showed in Figure 3 HOM-ACC decreased with NO_X, while HOM monomers remained about constant. We therefore analyze how a reduction of SOA could be realized when HOM monomers (here HOM-ON) are formed instead of HOMM-ACC. According to reaction R5, HOM accretion products are produced from two peroxy radicals (Berndt et al., 2018a, 2018b). The other product of this reaction is molecular oxygen and thus the molecular mass of the HOM accretion product is lower by 32 Da than the sum of the molecular masses of both monomer peroxy radicals. If two HOM-ON are formed from two HOM-RO_2 by reactions R6a and R7 instead of one HOM-ACC, each of them gains molecular mass due to the addition of NO (30 Da) or NO_2 (46 Da). Comparing the molecular mass of two HOM-ON to that of the HOM-ACC formed from the same HOM-RO_2, there may be even a gain of 92 Da to 124 Da when two HOM-ON are formed on cost of one HOM-ACC. This gain considers the addition of two NO or two NO_2 in the formation of HOM-ON and the loss of O_2 in HOM-ACC formation. Hence, if the respective HOM-ACC is formed by HOM-RO_2 radicals that anyhow would form low volatility HOM-ON, the suppression of HOM-ACC should actually lead to an increase of total condensable mass.

The situation is different if we assume that classical ("non SOA forming") RO_2 with lower O:C ratio were involved in HOM-ACC formation besides HOM-RO_2. If the RO_2 is not terminated by a HOM-RO_2 to HOM-ACC, the volatility of its classical termination products may be too high to allow for effective condensation and contribution to SOA formation. In such cases, HOM-ACC formation would lead to a gain of condensable mass by scavenging the "non SOA forming" peroxy radical. In

turn, suppression of HOM-ACC formation would indeed lead to a net loss of condensable mass. This effect is de facto the same as accretion product suppression by isoprene peroxy radicals described by McFiggans et al. (2019).

The loss could be even stronger when two intermediate level oxidized (functionalized) peroxy radicals are involved in the accretion product formation. If both form volatile termination products otherwise, the whole accretion product accounts for loss. Involvement of "non-SOA forming" RO_2 in HOM-ACC formation can be verified by looking at average O:C ratios derived from high resolution peak identification. For α-pinene at the background level of NO_X the average O:C is 0.97 for the monomers and 0.68 for the accretion products. The lower O:C ratios of HOM-ACC indicate a substantial contribution of RO_2 with smaller numbers of O atoms.

Since HOM-ACC can be formed from many permutations of HOM-RO_2 and "non-SOA forming" RO_2, clear identification of the respective precursors is not possible. Referring to rate coefficients reported by Berndt et al. (2018b), which decrease with the degree of functionalization by two orders of magnitude, we propose that there may be three types of pathways to accretion products: HOM-RO_2· + HOM-RO_2·, HOM-RO_2· + RO_2·, and RO_2· + RO_2·. Formation of accretion products by reaction HOM-RO_2· + RO_2· were observed for cyclopentene by Mentel et al. (2015). For illustration we simply assume that accretion product formation involves a pre-stabilized adduct (in analogy to the Lindemann-Hinshelwood mechanism). Then HOM-RO_2· + HOM-RO_2· would form a relatively long lived and relatively stable adduct because of the high functionalization of the reactants (with protic functional groups). Such adduct would live long enough to react to the accretion products e.g. as proposed by Valiev et al. (Chem. Comm., 2019). HOM-RO_2·+RO_2· form weaker adducts with shorter lifetimes, but there are more collisions to form adducts as [RO_2·] are higher than [HOM-RO_2·]. RO_2· + RO_2· may still take place, driven by bare number of collisions. All involved RO_2· must have certain degree of functionalization (Berndt et al. 2018a, b). First generation RO_2· contain only 3 O-atoms, but are by far the most abundant. Reactions of first generation peroxy radicals could therefore still make a contribution to accretion products.

We conclude that suppression of HOM accretion product formation is a mechanism that leads to lower amounts of condensable mass because of involvement of "non SOA forming" RO_2· and therefore can explain the suppressing effect of NO_X on SOA formation. Note that in the experiments here RO_2· dominated over HO_2·. This is often the case in laboratory studies with enhanced VOC and oxidant levels. Insofar, suppression of accretion products may well explain the dependence of SOA formation on NO_X (and the variability) observed in laboratory studies. In the atmosphere, photochemical accretion product formation at low NO_X can often be less important because termination reactions with HO_2 are more important for HOM formation than termination reactions with RO_2 (compare Berndt et al., 2018a for example of isoprene).

5 Summary and conclusion

We characterized the role of ON for SOA mass formation. One finding was that low functionalized ON do not contribute much to particle formation. Only HOM-ON with more than 6 O-atoms at the HOM moiety can efficiently contribute to SOA mass formation at least at mass loads as investigated here. Thereby HOM-ON with 6 to 7 O atoms showed partitioning with

γ_{eff} of about 0.5, i.e. about 50% staying in the particulate phase. Once the HOM-ON contained more than 8 O-atoms their loss on particles was collision limited and nearly 100% resided in the particulate phase. This supports expectations that HOM-ON with more than 8 O-atoms will have extreme low volatility. No significant and systematic differences in γ_{eff} were found between HOM-ON and HOM-PP when they have the same number of O-atoms in the moiety, i.e. when they arise from the same HOM-RO_2. Hence, different volatility of HOM-ON and HOM-PP from different termination reactions can be discarded as reason for the suppressing effect of NO_X on SOA mass formation. Hydrolysis of HOM-ON in the particle phase and re-evaporation of HNO_3 seems also insufficient to explain the suppressing impacts of NO_X on SOA mass formation. Re-evaporation of HNO_3 more or less just compensates the mass gain due to the formation of a HOM-ON instead of a HOM-PP. Thus we conclude that formation of HOM-ON instead of HOM-PP (i.e. hydroperoxides, -alcohols, -ketones, -carboxylic or -percarboxylic acids) cannot be the main reason for the often observed suppressing effect of NO_X on SOA formation in photochemical systems. Since a suppressing effect of NO_X on SOA mass formation is well documented in the literature (Presto et al., 2005; Kroll et al., 2006; Ng et al., 2007; Eddingsaas et al., 2012; Sarrafzadeh et al., 2016; Stirnweis et al., 2017), there must be other mechanisms causing this suppression. One effect is the lowering of the OH level by NO_X (e.g. Sarrafzadeh et al., 2016; Lee et al. 2020). If OH is kept constant, we observed strong suppression of HOM-ACC with increasing [NO_X]. Formation of HOM-ON via fast R6a, R7 in competition to R4a is probably the reason of the observed phenomenon, especially if R6a and R7 prevent that less functionalized RO_2 are trapped in low volatility accretion products. Without forming accretion product, there is no chance for them to participate in SOA mass formation because of the high volatility of their other termination products. Keeping off less functionalized HOM-RO_2 from forming accretion products leads to loss of one molecular mass unit of less functionalized RO_2 or even the whole accretion product if it was formed by two intermediate level oxidized peroxy radical. This effect may be less expressed in the atmosphere as RO_2 - RO_2 interactions in low NO_X cases are less important than in our laboratory study.

There is another contribution left for an explanation of SOA mass suppression by NO_X: the decomposition of alkoxy radicals that are formed in reaction R6b. We showed in Figure 3 that fragmentation of alkoxy radicals led to $C_{<10}$ compounds, that are still HOM that contribute to SOA. At the current stage the overall impact of alkoxy radicals on HOM and SOA formation is difficult to address and needs closer study (in preparation).

Note, that we considered the photochemistry of NO_X to SOA contribution for two major MT, α-pinene and β-pinene. We find that that SOA yields are fairly independent of NO_X, but drop significantly at the highest NO_X levels. Model studies show that increase of NO_X emissions may also lead to more SOA, when NO_3 is the oxidant (e.g. Pye et al. 2015) or when isoprene is involved (Marais et al. 2016). In the latter case NO directs the gas phase mechanism toward isoprene products with reactive uptake, while for compounds like α-pinene and β-pinene, investigated here, condensation is more important for SOA formation and thus vapor pressures controls SOA yields.

Data availability

All data given in figures can be displayed in tables or in digital form. This includes the data given in the Supplement where we describe methodological issues including calibrations, peak separation in CIMS, and peak lists. Please send all requests for data to t.mentel@fz-juelich.de.

Author contributions

TFM, JW, EK, IP, AW, and AKS designed the experiments. Instrument deployment and operation were carried out by IP, SS, MS, PS, SA, EK, FR, MS, RT, JW, CW, and DZ. Data analysis was done by IP, SK, SS, FR, PS, and RT. IP, SK, SS, JW and TFM interpreted the compiled data set. IP, SK, JW, TFM, and AKS wrote the paper. All co-authors discussed the results and commented on the paper.

Competing interests

Sebastian Schmitt is working for TSI GmbH. The authors declare that they have no conflict of interest.

Acknowledgements

This work was supported by the European Commission's 7th Framework Program under grant agreement no. 287382 (Marie Curie Training Network PIMMS).

References

Atkinson, R.: Gas-Phase Tropospheric Chemistry of Organic Compounds, J. Phys. Chem. Ref. Data, Monograph No. 2, 1994.

Atkinson, R.: Gas-Phase Tropospheric Chemistry of Volatile Organic Compounds: 1. Alkanes and Alkenes, J. Phys. Chem. Ref. Data, Vol. 26, No. 2, 215-290, doi: 10.1063/1.556012, 1997.

Bean, J. K., and Hildebrandt Ruiz, L.: Gas–particle partitioning and hydrolysis of organic nitrates formed from the oxidation of α-pinene in environmental chamber experiments, Atmos. Chem. Phys., 16, 2175-2016, doi:10.5194/acp-16-2175-2016, 2016.

Berkemeier, T., Ammann, M., Mentel, T. F., Poschl, U. and Shiraiwa, M.: Organic nitrate contribution to new particle formation and growth in secondary organic aerosols from α-pinene ozonolysis, Environ. Sci. Technol., 50, 6334-6342, doi: 10.1021/acs.est.6b00961, 2016.

Berndt, T., Richters, S., Jokinen, T., Hyttinen, N., Kurten, T., Otkjaer, R. V., Kjaergaard, H. G., Stratmann, F., Herrmann, H., Sipila, M., Kulmala, M., and Ehn, M.: Hydroxyl radical-induced formation of highly oxidized organic compounds, Nat. Comm., 7, 10.1038/ncomms13677, 2016.

Berndt, T., Mentler, B., Scholz, W., Fischer, L., Herrmann, H., Kulmala, M., and Hansel, A.: Accretion Product Formation from Ozonolysis and OH Radical Reaction of alpha-Pinene: Mechanistic Insight and the Influence of Isoprene and Ethylene, Environ. Sci. Techn., 52, 11069-11077, doi: 10.1021/acs.est.8b02210, 2018a.

Berndt, T., Scholz, W., Mentler, B., Fischer, L., Herrmann, H., Kulmala, M., and Hansel, A.: Accretion Product Formation from Self- and Cross-Reactions of RO2 Radicals in the Atmosphere, Angew. Chem.-International Edition, 57, 3820-3824, doi: 10.1002/anie.201710989, 2018b.

Bianchi, F., Tröstl, J., Junninen, H., Frege, C., Henne, S., Hoyle, C. R., Molteni, U., Herrmann, E., Adamov, A., Bukowiecki, N., Chen, X., Duplissy, J., Gysel, M., Hutterli, M., Kangasluoma, J., Kontkanen, J., Kurten, A., Manninen, H. E., Munch, S., Perakyla, O., Petaja, T., Rondo, L., Williamson, C., Weingartner, E., Curtius, J., Worsnop, D. R., Kulmala, M., Dommen, J., and Baltensperger, U.: New particle formation in the free troposphere: A question of chemistry and timing, Science, 352, 1109-1112, doi: 10.1126/science.aad5456, 2016.

Bianchi, F., Kurten, T., Riva, M., Mohr, C., Rissanen, M. P., Roldin, P., Berndt, T., Crounse, J. D., Wennberg, P. O., Mentel, T. F., Wildt, J., Junninen, H., Jokinen, T., Kulmala, M., Worsnop, D. R., Thornton, J. A., Donahue, N., Kjaergaard, H. G., and Ehn, M.: Highly Oxygenated Organic Molecules (HOM) from Gas-Phase Autoxidation Involving Peroxy Radicals: A Key Contributor to Atmospheric Aerosol, Chemical Reviews, 119, 3472-3509, doi: 10.1021/acs.chemrev.8b00395, 2019.

Boyd, C. M., Nah, T., Xu, L., Berkemeier, T., and Ng, N. L.: Secondary Organic Aerosol (SOA) from Nitrate Radical Oxidation of Monoterpenes: Effects of Temperature, Dilution, and Humidity on Aerosol Formation, Mixing, and Evaporation, Environ. Sci. Technol., 51, 7831-7841, 10.1021/acs.est.7b01460, 2017.

Boyd, C. M., Sanchez, J., Xu, L., Eugene, A. J., Nah, T., Tuet, W. Y., Guzman, M. I., and Ng, N. L.: Secondary organic aerosol formation from the β-pinene+NO_3 system: effect of humidity and peroxy radical fate, Atmos. Chem. Phys., 15, 7497-7522, doi: 10.5194/acp-15-7497-2015, 2015.

Breitenlechner, M., Fischer, L., Hainer, M., Heinritzi, M., Curtius, J. and Hansel, A.: PTR3: An Instrument for Studying the Lifecycle of Reactive Organic Carbon in the Atmosphere, Anal. Chem., 89, 5825-5832, doi: 10.1021/acs.analchem.6b05110, 2017.

Browne, E. C., Min, K. E., Wooldridge, P. J., Apel, E., Blake, D. R., Brune, W. H., Cantrell, C. A., Cubison, M. J., Diskin, G. S., Jimenez, J. L., Weinheimer, A. J., Wennberg, P. O., Wisthaler, A. and Cohen, R. C.: Observations of total

$RONO_2$ over the boreal forest: NO_X sinks and HNO_3 sources, Atmos. Chem. Phys., 13, 4543-4562, doi: 10.5194/acp-13-4543-2013, 2013.

Carlton, A. G., Pinder, R. W., Bhave, P. V., and Pouliot, G. A.: To What Extent Can Biogenic SOA be Controlled?, Environ. Sci. Techn., 44, 3376-3380, doi: 10.1021/es903506b, 2010.

Capouet, M. and Müller, J. F.: A group contribution method for estimating the vapour pressures of alpha-pinene oxidation products, Atmos. Chem. Phys., 6, 1455-1467, doi: 10.5194/acp-6-1455-2006, 2006.

Claflin, M. S., and Ziemann, P. J.: Identification and Quantitation of Aerosol Products of the Reaction of beta-Pinene with NO_3 Radicals and Implications for Gas- and Particle-Phase Reaction Mechanisms, J. Phys. Chem. A, 122, 3640-3652, 10.1021/acs.jpca.8b00692, 2018.

Crounse, J. D., Paulot, F., Kjaergaard, H. G., and Wennberg, P. O.: Peroxy radical isomerization in the oxidation of isoprene, Phys. Chem. Chem. Phys., 13, 13607-13613, doi: 10.1039/c1cp21330j, 2011.

Day, D. A., Liu, S., Russell, L. M., and Ziemann, P. J.: Organonitrate group concentrations in submicron particles with high nitrate and organic fractions in coastal southern California, Atmos. Environ., 44, 1970–1979, doi:10.1016/j.atmosenv.2010.02.045, 2010.

Eddingsaas, N. C., Loza, C. L., Yee, L. D., Chan, M., Schilling, K. A., Chhabra, P. S., Seinfeld, J. H. and Wennberg, P. O.: alpha-pinene photo-oxidation under controlled chemical conditions - Part 2: SOA yield and composition in low- and high-NOx environments, Atmos. Chem. Phys., 12, 7413-7427, doi: 10.5194/acp-12-7413-2012, 2012.

Ehn, M., Kleist, E., Junninen, H., Petaja, T., Lonn, G., Schobesberger, S., Dal Maso, M., Trimborn, A., Kulmala, M., Worsnop, D. R., Wahner, A., Wildt, J. and Mentel, T. F.: Gas phase formation of extremely oxidized pinene reaction products in chamber and ambient air, Atmos. Chem. Phys., 12(11), 5113–5127, doi:10.5194/acp-12-5113-2012, 2012.

Ehn, M., Thornton, J. A., Kleist, E., Sipilä, M., Junninen, H., Pullinen, I., Springer, M., Rubach, F., Tillmann, R., Lee, B., Lopez-Hilfiker, F., Andres, S., Acir, I.-H., Rissanen, M., Jokinen, T., Schobesberger, S., Kangasluoma, J., Kontkanen, J., Nieminen, T., Kurtén, T., Nielsen, L. B., Jørgensen, S., Kjaergaard, H. G., Canagaratna, M., Dal Maso, M., Berndt, T., Petäjä, T., Wahner, A., Kerminen,V.-M., Kulmala, M., Worsnop, D. R., Wildt, J., and Mentel, T. F.: A large source of low-volatility secondary organic aerosol, Nature, 506, 476–479, doi:10.1038/nature13032, 2014.

Ehn, M., Berndt, T., Wildt, J., and Mentel, T.: Highly Oxygenated Molecules from Atmospheric Autoxidation of Hydrocarbons: A Prominent Challenge for Chemical Kinetics Studies, International Journal of Chemical Kinetics, 49, 821-831, doi: 10.1002/kin.21130, 2017.

Emanuelsson, E. U., Hallquist, M., Kristensen, K., Glasius, M., Bohn, B., Fuchs, H., Kammer, B., Kiendler-Scharr, A., Nehr, S., Rubach, F., Tillmann, R., Wahner, A., Wu, H. C. and Mentel, T. F.: Formation of anthropogenic secondary organic aerosol (SOA) and its influence on biogenic SOA properties, Atmos. Chem. Phys., 13, 2837-2855, doi: 10.5194/acp-13-2837-2013, 2013.

Farmer, D. K., Matsunaga, A., Docherty, K. S., Surratt, J. D., Seinfeld, J. H., Ziemann, P. J. and Jimenez, J. L.: Response of an aerosol mass spectrometer to organonitrates and organosulfates and implications for atmospheric chemistry, Proc. Natl. Acad. Sci. U.S.A., 107, 6670-6675, doi: 10.1073/pnas.0912340107, 2010.

Faxon, C., Hammes, J., Le Breton, M., Pathak, R. K., and Hallquist, M.: Characterization of organic nitrate constituents of secondary organic aerosol (SOA) from nitrate-radical-initiated oxidation of limonene using high-resolution chemical ionization mass spectrometry, Atmos. Chem. Phys., 18, 5467-5481, 10.5194/acp-18-5467-2018, 2018.

Fisher, J. A., Jacob, D. J., Travis, K. R., Kim, P. S., Marais, E. A., Chan Miller, C., Yu, K., Zhu, L., Yantosca, R. M., Sulprizio, M. P., Mao, J., Wennberg, P. O., Crounse, J. D., Teng, A. P., Nguyen, T. B., St. Clair, J. M., Cohen, R. C., Romer, P., Nault, B. A., Wooldridge, P. J., Jimenez, J. L., Campuzano-Jost, P., Day, D. A., Hu, W., Shepson, P. B., Xiong, F., Blake, D. R., Goldstein, A. H., Misztal, P. K., Hanisco, T. F., Wolfe, G. M., Ryerson, T. B., Wisthaler, A., and Mikoviny, T.: Organic nitrate chemistry and its implications for nitrogen budgets in an isoprene- and monoterpene-rich atmosphere: constraints from aircraft (SEAC4RS) and ground-based (SOAS) observations in the Southeast US, Atmos. Chem. Phys., 16, 5969-5991, 10.5194/acp-16-5969-2016, 2016.

Fry, J. L., Draper, D. C., Zarzana, K. J., Campuzano-Jost, P., Day, D. A., Jimenez, J. L., Brown, S. S., Cohen, R. C., Kaser, L., Hansel, A., Cappellin, L., Karl, T., Roux, A. H., Turnipseed, A., Cantrell, C., Lefer, B. L. and Grossberg, N.: Observations of gas- and aerosol-phase organic nitrates at BEACHON-RoMBAS 2011, Atmos. Chem. Phys., 13, 8585-8605, doi: 10.5194/acp-13-8585-2013, 2013.

Fry, J. L., Draper, D. C., Barsanti, K. C., Smith, J. N., Ortega, J., Winkle, P. M., Lawler, M. J., Brown, S. S., Edwards, P. M., Cohen, R. C. and Lee, L.: Secondary Organic Aerosol formation and organic nitrate yield from NO_3 oxidation of biogenic hydrocarbons, Environ. Sci. Technol., 48, 11944-11953, doi: 10.1021/es502204x, 2014.

Fuchs, N. A., Sutugin, A. G., Hidy, G. M., and Brock, J. R.: High-dispersed aerosols, Topics in Current Aerosol Research, 2, 1-60, doi.org/10.1016/B978-0-08-016674-2.50006-6, 1971.

Fuller, E. N., Ensley, K., and Giddings, J. C.: Diffusion of halogenated hydrocarbons in helium. Effect of structure on collision cross sections, J. Phys. Chem., 73, 3679- 3685, doi: 10.1021/j100845a020, 1969.

Glasius, M., la Cour, A. and Lohse, C.: Fossil and nonfossil carbon in fine particulate matter: A study of five European cities, J. Geophys. Res. Atmos., 116, D11302, doi: 10.1029/2011JD015646, 2011.

de Gouw, J. A., Middlebrook, A. M., Warneke, C., Goldan, P. D., Kuster, W. C., Roberts, J. M., Fehsenfeld, F. C., Worsnop, D. R., Canagaratna, M. R., Pszenny, A. A. P., Keene, W. C., Marchewka, M., Bertman, S. B., and Bates, T. S.: Budget of organic carbon in a polluted atmosphere: Results from the New England Air Quality Study in 2002, J. Geophys. Res. Atmos., 110, D16305, doi: 10.1029/2004jd005623, 2005

Guenther, A. B., Jiang, X., Heald, C. L., Sakulyanontvittaya, T., Duhl, T., Emmons, L. K., and Wang, X.: The Model of Emissions of Gases and Aerosols from Nature version 2.1 (MEGAN2.1): an extended and updated framework for modeling biogenic emissions, Geosci. Model Dev., 5, 1471–1492, doi:10.5194/gmd-51471-2012, 2012.

Hallquist, M., Wenger, J. C., Baltensperger, U., Rudich, Y., Simpson, D., Claeys, M., Dommen, J., Donahue, N. M., George, C., Goldstein, A. H., Hamilton, J. F., Herrmann, H., Hoffmann, T., Iinuma, Y., Jang, M., Jenkin, M. E., Jimenez, J. L., Kiendler-Scharr, A., Maenhaut, W., McFiggans, G., Mentel, T. F., Monod, A., Prevot, A. S. H., Seinfeld, J. H., Surratt, J. D., Szmigielski, R. and Wildt, J.: The formation, properties and impact of secondary organic aerosol: current and emerging issues, Atmos. Chem. Phys., 9, 5155-5236, doi: 10.5194/acp-9-5155-2009, 2009.

Han, Y. M., Stroud, C. A., Liggio, J. and Li, S. M.: The effect of particle acidity on secondary organic aerosol formation from alpha-pinene photooxidation under atmospherically relevant conditions, Atmos. Chem. Phys., 16, 13929-13944, doi: 10.5194/acp-16-13929-2016, 2016.

Hoyle, C. R., Boy, M., Donahue, N. M., Fry, J. L., Glasius, M., Guenther, A., Hallar, A. G., Hartz, K. H., Petters, M. D., Petaja, T., Rosenoern, T. and Sullivan, A. P.: A review of the anthropogenic influence on biogenic secondary organic aerosol, Atmos. Chem. Phys., 11, 321-343, doi: 10.5194/acp-11-321-2011, 2011.

Hu, K. S., Darer, A. I., and Elrod, M. J.: Thermodynamics and kinetics of the hydrolysis of atmospherically relevant organonitrates and organosulfates, Atmos. Chem. and Phys., 11, 8307-8320, 10.5194/acp-11-8307-2011, 2011.

Hyttinen, N., Rissanen, M. P., and Kurten, T.: Computational Comparison of Acetate and Nitrate Chemical Ionization of Highly Oxidized Cyclohexene Ozonolysis Intermediates and Products, Journal of Physical Chemistry A, 121, 2172-2179, doi: 10.1021/acs.jpca.6b12654, 2017

Jacobs, M. I., Burke, W. J., and Elrod, M. J.: Kinetics of the reactions of isoprene-derived hydroxynitrates: gas phase epoxide formation and solution phase hydrolysis, Atmos. Chem. Phys., 14, 8933–8946, doi:10.5194/acp-14-8933-2014, 2014.

Jokinen, T., Berndt, T., Makkonen, R., Kerminen, V. M., Junninen, H., Paasonen, P., Stratmann, F., Herrmann, H., Guenther, A. B., Worsnop, D. R., Kulmala, M., Ehn, M. and Sipila, M.: Production of extremely low volatile organic compounds from biogenic emissions: Measured yields and atmospheric implications, Proc. Natl. Acad. Sci. U.S.A., 112, 7123-7128, doi: 10.1073/pnas.1423977112, 2015.

Kiendler-Scharr, A., Mensah, A. A., Friese, E., Topping, D., Nemitz, E., Prevot, A. S. H., Äijälä, M., Allan, J., Canonaco, F., Canagaratna, M., Carbone S., Crippa, M., Dall Osto, M., Day, D. A., De Carlo, P., Di Marco, C. F., Elbern, H., Eriksson, A., Freney, E., Hao, L., Herrmann, H., Hildebrandt, L., Hillamo, R., Jimenez, J. L., Laaksonen, A., McFiggans, G., Mohr, C., O'Dowd, C., Otjes, R., Ovadnevaite, J., Pandis, S. N., Poulain, L., Schlag, P., Sellegri, K., Swietlicki, E., Tiitta, P., Vermeulen, A., Wahner, A., Worsnop, D., and Wu, H.-C.: Ubiquity of organic nitrates from nighttime chemistry in the European submicron aerosol, Geophys. Res. Lett., 43, 7735 – 7744, doi:10.1002/2016GL069239, 2016.

Kim, H., Barkey, B. and Paulson, S. E.: Real Refractive Indices and Formation Yields of Secondary Organic Aerosol Generated from Photooxidation of Limonene and alpha-Pinene: The Effect of the HC/NO_X Ratio, J. Phys. Chem. A, 116, 6059-6067, doi: 10.1021/jp301302z, 2012.

Kirkby, J., Duplissy, J., Sengupta, K., Frege, C., Gordon, H., Williamson, C., Heinritzi, M., Simon, M., Yan, C., Almeida, J., Tröstl, J., Nieminen, T., Ortega, I. K., Wagner, R., Adamov, A., Amorim, A., Bernhammer, A. K., Bianchi, F., Breitenlechner, M., Brilke, S., Chen, X. M., Craven, J., Dias, A., Ehrhart, S., Flagan, R. C., Franchin, A., Fuchs, C., Guida, R., Hakala, J., Hoyle, C. R., Jokinen, T., Junninen, H., Kangasluoma, J., Kim, J., Krapf, M., Kurten,?? A., Laaksonen, A., Lehtipalo, K., Makhmutov, V., Mathot, S., Molteni, U., Onnela, A., Perakyla, O., Piel, F., Petaja, T., Praplan, A. P., Pringle, K., Rap, A., Richards, N. A. D., Riipinen, I., Rissanen, M. P., Rondo, L., Sarnela, N., Schobesberger, S., Scott, C. E., Seinfeld, J. H., Sipila, M., Steiner, G., Stozhkov, Y., Stratmann, F., Tome, A., Virtanen, A., Vogel, A. L., Wagner, A. C., Wagner, P. E., Weingartner, E., Wimmer, D., Winkler, P. M., Ye, P. L., Zhang, X., Hansel, A., Dommen, J., Donahue, N. M., Worsnop, D. R., Baltensperger, U., Kulmala, M., Carslaw, K. S., Curtius, J.: Ion-induced nucleation of pure biogenic particles, Nature, 533, 521−526, doi: 10.1038/nature17953, 2016.

Kroll, J. H., Ng, N. L., Murphy, S. M., Flagan, R. C. and Seinfeld, J. H.: Secondary organic aerosol formation from isoprene photo-oxidation, Environ. Sci. Technol., 40, 1869-1877, doi: 10.1021/es0524301, 2006.

Lee, A. K. Y., Abbatt, J. P. D., Leaitch, W. R., Li, S. M., Sjostedt, S. J., Wentzell, J. J. B., Liggio, J., and Macdonald, A. M.: Substantial secondary organic aerosol formation in a coniferous forest: observations of both day- and nighttime chemistry, Atmos. Chem. Phys., 16, 6721-6733, doi: 10.5194/acp-16-6721-2016, 2016a.

Lee, B., D'Ambro, E. L., Lopez-Hilfiker, F. D., Schobesberger, S., Mohr, C., Zawadowicz, M. A., Liu, J. M., Shilling, J. E., Hu, W. W., Palm, B. B., Jimenez, J. L., Hao, L. Q., Virtanen, A., Zhang, H. F., Goldstein, A. H., Pye, H. O. T., and Thornton, J. A.: Resolving Ambient Organic Aerosol Formation and Aging Pathways with Simultaneous Molecular Composition and Volatility Observations, ACSEarthSpaceChem., 4, 391-402, doi: 10.1021/acsearthspacechem.9b00302, 2020.

Lee, B. H., Mohr, C., Lopez-Hilfiker, F. D., Lutz, A., Hallquist, M., Lee, L., Romer, P., Cohen, R. C., Iyer, S., Kurten, T., Hu, W. W., Day, D. A., Campuzano-Jost, P., Jimenez, J. L., Xu, L., Ng, N. L., Guo, H. Y., Weber, R. J., Wild, R. J., Brown, S. S., Koss, A., de Gouw, J., Olson, K., Goldstein, A. H., Seco, R., Kim, S., McAvey, K., Shepson, P. B., Starn, T., Baumann, K., Edgerton, E. S., Liu, J. M., Shilling, J. E., Miller, D. O., Brune, W., Schobesberger, S., D'Ambro, E. L. and Thornton, J. A.: Highly functionalized organic nitrates in the southeast United States: Contribution to secondary organic aerosol and reactive nitrogen budgets, Proc. Natl. Acad. Sci. U.S.A., 113, 1516-1521, doi: 10.1073/pnas.1508108113, 2016b.

Lehtipalo, K., Yan, C., Dada, L., Bianchi, F., Xiao, M., Wagner, R., Stolzenburg, D., Ahonen, L. R., Amorim, A., Baccarini, A., Bauer, P. S., Baumgartner, B., Bergen, A., Bernhammer, A. K., Breitenlechner, M., Brilke, S., Buchholz, A., Mazon, S. B., Chen, D. X., Chen, X. M., Dias, A., Dommen, J., Draper, D. C., Duplissy, J., Ehn, M., Finkenzeller, H., Fischer, L., Frege, C., Fuchs, C., Garmash, O., Gordon, H., Hakala, J., He, X. C., Heikkinen, L., Heinritzi, M., Helm, J. C., Hofbauer, V., Hoyle, C. R., Jokinen, T., Kangasluoma, J., Kerminen, V. M., Kim, C., Kirkby, J., Kontkanen, J., Kurten, A., Lawler, M. J., Mai, H. J., Mathot, S., Mauldin, R. L., Molteni, U., Nichman, L., Nie, W.,

Nieminen, T., Ojdanic, A., Onnela, A., Passananti, M., Petaja, T., Piel, F., Pospisilova, V., Quelever, L. L. J., Rissanen, M. P., Rose, C., Sarnela, N., Schallhart, S., Schuchmann, S., Sengupta, K., Simon, M., Sipila, M., Tauber, C., Tome, A., Trostl, J., Vaisanen, O., Vogel, A. L., Volkamer, R., Wagner, A. C., Wang, M. Y., Weitz, L., Wimmer, D., Ye, P. L., Ylisirnio, A., Zha, Q. Z., Carslaw, K. S., Curtius, J., Donahue, N. M., Flagan, R. C., Hansel, A., Riipinen, I., Virtanen, A., Winkler, P. M., Baltensperger, U., Kulmala, M., and Worsnop, D. R.: Multicomponent new particle formation from sulfuric acid, ammonia, and biogenic vapors, Science Advances, 4, doi: 10.1126/sciadv.aau5363, 2018.

Liu, S., Shilling, J. E., Song, C., Hiranuma, N., Zaveri, R. A., and Russell, L. M.: Hydrolysis of organonitrate functional groups in aerosol particles, Aerosol Sci. Tech., 46, 1359–1369, doi:10.1080/02786826.2012.716175, 2012.

Marais, E. A., Jacob, D. J., Jimenez, J. L., Campuzano-Jost, P., Day, D. A., Hu, W., Krechmer, J., Zhu, L., Kim, P. S., Miller, C. C., Fisher, J. A., Travis, K., Yu, K., Hanisco, T. F., Wolfe, G. M., Arkinson, H. L., Pye, H. O. T., Froyd, K. D., Liao, J., and McNeill, V. F.: Aqueous-phase mechanism for secondary organic aerosol formation from isoprene: application to the southeast United States and co-benefit of SO2 emission controls, Atmos. Chem. Phys., 16, 1603-1618, 10.5194/acp-16-1603-2016, 2016.

McFiggans, G., Mentel, T. F., Wildt, J., Pullinen, I., Kang, S., Kleist, E., Schmitt, S., Springer, M., Tillmann, R., Wu, C., Zhao, D., Hallquist, M., Faxon, C., Le Breton, M., Hallquist, Å. M., Simpson, D., Bergström, R., Jenkin, M. E., Ehn, M., Thornton, J. A., Alfarra, M. R., Bannan, T. J., Percival, C. J., Priestley, M., Topping, D., and Kiendler-Scharr, A.: Secondary organic aerosol reduced by mixture of atmospheric vapours, Nature, 565, 587-593, doi: 10.1038/s41586-018-0871-y, 2019.

Mentel, T. F., Wildt, J., Kiendler-Scharr, A., Kleist, E., Tillmann, R., Dal Maso, M., Fisseha, R., Hohaus, T., Spahn, H., Uerlings, R., Wegener, R., Griffiths, P. T., Dinar, E., Rudich, Y. and Wahner, A.: Photochemical production of aerosols from real plant emissions, Atmos. Chem. Phys., 9, 4387-4406, doi: 10.5194/acpd-9-3041-2009, 2009.

Mentel, T. F., Kleist, E., Andres, S., Dal Maso, M., Hohaus, T., Kiendler-Scharr, A., Rudich, Y., Springer, M., Tillmann, R., Uerlings, R., Wahner, A. and Wildt, J.: Secondary aerosol formation from stress-induced biogenic emissions and possible climate feedbacks, Atmos. Chem. Phys., 13, 8755-8770, doi: 10.5194/acp-13-8755-2013, 2013.

Mentel, T. F., Springer, M., Ehn, M., Kleist, E., Pullinen, I., Kurtén, T., Rissanen, M., Wahner, A., and Wildt, J.: Formation of highly oxidized multifunctional compounds: autoxidation of peroxy radicals formed in the ozonolysis of alkenes – deduced from structure-product relationships, Atmos. Chem. Phys., 15, 6745– 6765, doi:10.5194/acp-15-6745-2015, 2015.

Mutzel, A., Poulain, L., Berndt, T., Iinuma, Y., Rodigast, M., Boge, O., Richters, S., Spindler, G., Sipila, M., Jokinen, T., Kulmala, M. and Herrmann, H.: Highly Oxidized Multifunctional Organic Compounds Observed in Tropospheric Particles: A Field and Laboratory Study, Environ. Sci. Technol., 49, 7754-7761, doi: 10.1021/acs.est.5b00885, 2015.

Ng, N. L., Brown, S. S., Archibald, A. T., Atlas, E., Cohen, R. C., Crowley, J. N., Day, D. A., Donahue, N. M., Fry, J. L., Fuchs, H., Griffin, R. J., Guzman, M. I., Herrmann, H., Hodzic, A., Iinuma, Y., Jimenez, J. L., Kiendler-Scharr, A., Lee, B. H., Luecken, D. J., Mao, J., McLaren, R., Mutzel, A., Osthoff, H. D., Ouyang, B., Picquet-Varrault, B., Platt, U., Pye, H. O. T., Rudich, Y., Schwantes, R. H., Shiraiwa, M., Stutz, J., Thornton, J. A., Tilgner, A., Williams, B. J., and Zaveri, R. A.: Nitrate radicals and biogenic volatile organic compounds: oxidation, mechanisms, and organic aerosol, Atmos. Chem. Phys., 17, 2103-2162, 10.5194/acp-17-2103-2017, 2017.

Ng, N. L., Chhabra, P. S., Chan, A. W. H., Surratt, J. D., Kroll, J. H., Kwan, A. J., McCabe, D. C., Wennberg, P. O., Sorooshian, A., Murphy, S. M., Dalleska, N. F., Flagan, R. C. and Seinfeld, J. H.: Effect of NO_X level on secondary organic aerosol (SOA) formation from the photo-oxidation of terpenes, Atmos. Chem. Phys., 7, 5159-5174, doi: 10.5194/acpd-7-10131-2007, 2007.

Noziere, B., Barnes, I. and Becker, K. H.: Product study and mechanisms of the reactions of alpha-pinene and of pinonaldehyde with OH radicals. J. Geophys. Res. Atmos., 104, 23645− 23656, doi: 10.1029/1999JD900778, 1999.

Pandis, S. N., Paulson, S. E., Seinfeld, J. H. and Flagan, R. C.: Aerosol formation in the photo-oxidation of isoprene and β-pinene, Atmos. Environ. Part A, 25, 997-1008, doi: 10.1016/0960-1686(91)90141-S, 1991.

Pankow, J. F. and Asher, W. E.: SIMPOL.1: a simple group contribution method for predicting vapor pressures and enthalpies of vaporization of multifunctional organic compounds, Atmos. Chem. Phys., 8, 2773–2796, doi:10.5194/acp-8-27732008, 2008.

Peräkylä, O., Riva, M., Heikkinen, L., Quéléver, L., Roldin, P., and Ehn, M.: Experimental investigation into the volatilities of highly oxygenated organic molecules (HOM), Atmos. Chem. Phys. Discuss., 2019, 1-28, doi: 10.5194/acp-2019-620, 2019.

Presto, A. A., Hartz, K. E. H., and Donahue, N. M.: Secondary organic aerosol production from terpene ozonolysis. 2. Effect of NOx concentration, Environ. Sci. Techn., 39, 7046-7054, 10.1021/es050400s, 2005.

Pullinen, I.: Photochemistry of Highly Oxidized Multifunctional Organic Molecules: a Chamber Study, Mathematisch-Naturwissenschaftliche Fakultät, Köln, Schriften des Forschungszentrums Jülich Reihe Energie & Umwelt / Energy & Environment, 2017.

Pye, H. O. T., Luecken, D. J., Xu, L., Boyd, C. M., Ng, N. L., Baker, K. R., Ayres, B. R., Bash, J. O., Baumann, K., Carter, W. P. L., Edgerton, E., Fry, J. L., Hutzell, W. T., Schwede, D. B., and Shepson, P. B.: Modeling the Current and Future Roles of Particulate Organic Nitrates in the Southeastern United States, Environmental Science & Technology, 49, 14195-14203, 10.1021/acs.est.5b03738, 2015.

Rindelaub, J. D., McAvey, K. M., and Shepson, P. B.: The photochemical production of organic nitrates from α-pinene and loss via acid-dependent particle phase hydrolysis, Atmos. Environ., 100, 193–201, doi:10.1016/j.atmosenv.2014.11.010, 2015.

Rindelaub, J. D., Borca, C. H., Hostetler, M. A., Slade, J. H., Lipton, M. A., Slipchenko, L. V. and Shepson, P. B.: The acid-catalyzed hydrolysis of an alpha-pinene-derived organic nitrate: kinetics, products, reaction mechanisms, and atmospheric impact, Atmos. Chem. Phys., 16, 15425-15432, doi: 10.5194/acp-16-15425-2016, 2016.

Rissanen, M. P.: NO2 Suppression of Autoxidation–Inhibition of Gas-Phase Highly Oxidized Dimer Product Formation, ACSEarthSpace Chem., 2, 1211-1219, doi: 10.1021/acsearthspacechem.8b00123, 2018.

Rissanen, M. P., Kurten, T., Sipilä, M., Thornton, J. A., Kangasluoma, J., Sarnela, N., Junninen, H., Jorgensen, S., Schallhart, S., Kajos, M. K., Taipale, R., Springer, M., Mentel, T. F., Ruuskanen, T., Petaja, T., Worsnop, D. R., Kjaergaard, H. G., and Ehn, M.: The Formation of Highly Oxidized Multifunctional Products in the Ozonolysis of Cyclohexene, Journal of the American Chemical Society, 136, 15596-15606, doi: 10.1021/ja507146s, 2014.

Riva, M., Rantala, P., Krechmer, J. E., Perakyla, O., Zhang, Y. J., Heikkinen, L., Garmash, O., Yan, C., Kulmala, M., Worsnop, D., and Ehn, M.: Evaluating the performance of five different chemical ionization techniques for detecting gaseous oxygenated organic species, Atmospheric Measurement Techniques, 12, 2403-2421, 10.5194/amt-12-2403-2019, 2019.

Rollins, A. W., Smith, J. D., Wilson, K. R. and Cohen, R. C.: Real time in situ detection of organic nitrates in atmospheric aerosols. Environ. Sci. Technol., 44 , doi: 10.1021/es100926x, 5540−5545, 2010.

Romer, P. S., Duffey, K. C., Wooldridge, P. J., Allen, H. M., Ayres, B. R., Brown, S. S., Brune, W. H., Crounse, J. D., de Gouw, J., Draper, D. C., Feiner, P. A., Fry, J. L., Goldstein, A. H., Koss, A., Misztal, P. K., Nguyen, T. B., Olson, K., Teng, A. P., Wennberg, P. O., Wild, R. J., Zhang, L. and Cohen, R. C.: The lifetime of nitrogen oxides in an isoprene-dominated forest, Atmos. Chem. Phys., 16, 7623-7637, doi: 10.5194/acp-16-7623-2016, 2016.

Rubach, F.: Aerosol processes in the Planetary Boundary Layer: High resolution Aerosol Mass Spectrometry on a Zeppelin NT Airship, Fachgruppe Chemie und Biologie, Physikalische und Theoretische Chemie, , Universität Wuppertal, Schriften des Forschungszentrums Jülich, Reihe Energie & Umwelt / Energy & Environment, Band / Volume 196, 2013.

Sarrafzadeh, M., Wildt, J., Pullinen, I., Springer, M., Kleist, E., Tillmann, R., Schmitt, S. H., Wu, C., Mentel, T. F., Zhao, D., Hastie, D. R. and Kiendler-Scharr, A.: Impact of NO_X and OH on secondary organic aerosol formation from β-pinene photo-oxidation, Atmos. Chem. Phys., 16, 11237-11248, doi: 10.5194/acp-16-11237-2016, 2016.

Shilling, J. E., Zaveri, R. A., Fast, J. D., Kleinman, L., Alexander, M. L., Canagaratna, M. R., Fortner, E., Hubbe, J. M., Jayne, J. T., Sedlacek, A., Setyan, A., Springston, S., Worsnop, D. R. and Zhang, Q.: Enhanced SOA formation from mixed anthropogenic and biogenic emissions during the CARES campaign, Atmos. Chem. Phys., 13, 2091-2113, doi: 10.5194/acp-13-2091-2013, 2013.

Spracklen, D. V., Jimenez, J. L., Carslaw, K. S., Worsnop, D. R., Evans, M. J., Mann, G. W., Zhang, Q., Canagaratna, M. R., Allan, J., Coe, H., McFiggans, G., Rap, A., and Forster, P.: Aerosol mass spectrometer constraint on the global secondary organic aerosol budget, Atmos. Chem. Phys., 11, 12109-12136, doi: 10.5194/acp-11-12109-2011, 2011

Stirnweis, L., Marcolli, C., Dommen, J., Barmet, P., Frege, C., Platt, S. M., Bruns, E. A., Krapf, M., Slowik, J. G., Wolf, R., Prévôt, A. S. H., Baltensperger, U. and El-Haddad, I.: Assessing the influence of NOx concentrations and relative humidity on secondary organic aerosol yields from α -pinene photo-oxidation through smog chamber experiments and modelling calculations, Atmos. Chem. Phys., 17, 5035-5061, doi: 10.5194/acp-17-5035-2017, 2017.

Takeuchi, M., and Ng, N. L.: Chemical composition and hydrolysis of organic nitrate aerosol formed from hydroxyl and nitrate radical oxidation of α-pinene and β-pinene, Atmos. Chem. Phys., 19, 12749-12766, 10.5194/acp-19-12749-2019, 2019.

Tröstl, J., Chuang, W. K., Gordon, H., Heinritzi, M., Yan, C., Molteni, U., Ahlm, L., Frege, C., Bianchi, F., Wagner, R., Simon, M., Lehtipalo, K., Williamson, C., Craven, J. S., Duplissy, J., Adamov, A., Almeida, J., Bernhammer, A. K., Breitenlechner, M., Brilke, S., Dias, A., Ehrhart, S., Flagan, R. C., Franchin, A., Fuchs, C., Guida, R., Gysel, M., Hansel, A., Hoyle, C. R., Jokinen, T., Junninen, H., Kangasluoma, J., Keskinen, H., Kim, J., Krapf, M., Kurten, A., Laaksonen, A., Lawler, M., Leiminger, M., Mathot, S., Mohler, O., Nieminen, T., Onnela, A., Petaja, T., Piel, F. M., Miettinen, P., Rissanen, M. P., Rondo, L., Sarnela, N., Schobesberger, S., Sengupta, K., Sipila, M., Smith, J. N., Steiner, G., Tome, A., Virtanen, A., Wagner, A. C., Weingartner, E., Wimmer, D., Winkler, P. M., Ye, P. L., Carslaw, K. S., Curtius, J., Dommen, J., Kirkby, J., Kulmala, M., Riipinen, I., Worsnop, D. R., Donahue, N. M., and Baltensperger, U.: The role of low-volatility organic compounds in initial particle growth in the atmosphere, Nature, 533, 527-531, doi: 10.1038/nature18271, 2016.

Wildt, J., Mentel, T. F., Kiendler-Scharr, A., Hoffmann, T., Andres, S., Ehn, M., Kleist, E., Muesgen, P., Rohrer, F., Rudich, Y., Springer, M., Tillmann, R. and Wahner, A.: Suppression of new particle formation from monoterpene oxidation by NO_X, Atmos. Chem. Phys., 14, 2789–2804, doi:10.5194/acp-14-2789-2014, 2014.

Worton, D. R., Goldstein, A. H., Farmer, D. K., Docherty, K. S., Jimenez, J. L., Gilman, J. B., Kuster, W. C., de Gouw, J., Williams, B. J., Kreisberg, N. M., Hering, S. V., Bench, G., McKay, M., Kristensen, K., Glasius, M., Surratt, J. D. and Seinfeld, J. H.: Origins and composition of fine atmospheric carbonaceous aerosol in the Sierra Nevada Mountains, California, Atmos. Chem. Phys., 11, 10219-10241, doi: 10.5194/acp-11-10219-2011, 2011.

Valiev, R. R., Hasan, G., Salo, V. T., Kubecka, J., and Kurten, T.: Intersystem Crossings Drive Atmospheric Gas-Phase Dimer Formation, J. Phys. Chem. A, 123, 6596-6604, 10.1021/acs.jpca.9b02559, 2019.

Vereecken, L., and Peeters, J.: Decomposition of substituted alkoxy radicals-part I: a generalized structure-activity relationship for reaction barrier heights, Phys. Chem. Chem. Phys., 11, 9062-9074, 10.1039/b909712k, 2009.

Vereecken, L., and Peeters, J.: A structure-activity relationship for the rate coefficient of H-migration in substituted alkoxy radicals, Phys. Chem. Chem. Phys., 12, 12608-12620, 10.1039/c0cp00387e, 2010.

Xu, L., Guo, H. Y., Boyd, C. M., Klein, M., Bougiatioti, A., Cerully, K. M., Hite, J. R., Isaacman-VanWertz, G., Kreisberg, N. M., Knote, C., Olson, K., Koss, A., Goldstein, A. H., Hering, S. V., de Gouw, J., Baumann, K., Lee, S. H., Nenes, A., Weber, R. J. and Ng, N. L.: Effects of anthropogenic emissions on aerosol formation from isoprene and

monoterpenes in the southeastern United States, Proc. Natl. Acad. Sci. U.S.A., 112, 37-42, doi: 10.1073/pnas.1417609112, 2015a.

Xu, L., Suresh, S., Guo, H., Weber, R. J. and Ng, N. L.: Aerosol characterization over the southeastern United States using high resolution aerosol mass spectrometry: spatial and seasonal variation of aerosol composition and sources with a focus on organic nitrates. Atmos. Chem. Phys., 15, 7307−7336 , doi: 10.5194/acp-15-7307-2015, 2015b.

Zhang, J. Y., Hartz, K. E. H., Pandis, S. N. and Donahue, N. M.: Secondary organic aerosol formation from limonene ozonolysis: Homogeneous and heterogeneous influences as a function of NO_X, J. Phys. Chem. A, 110, 11053-11063, doi: 10.1021/jp062836f, 2006.

Zhang, X., Lambe, A. T., Upshur, M. A., Brooks, W. A., Be, A. G., Thomson, R. J., Geiger, F. M., Surratt, J. D., Zhang, Z. F., Gold, A., Graf, S., Cubison, M. J., Groessl, M., Jayne, J. T., Worsnop, D. R. and Canagaratna, M. R.: Highly Oxygenated Multifunctional Compounds in alpha-Pinene Secondary Organic Aerosol, Environ. Sci. Technol., 51, 5932-5940, doi: 10.1021/acs.est.6b06588, 2017.

Zhao, D., Schmitt, S. H., Wang, M., Acir, I. H., Tillmann, R., Tan, Z., Novelli, A., Fuchs, H., Pullinen, I., Wegener, R., Rohrer, F., Wildt, J., Kiendler-Scharr, A., Wahner, A., and Mentel, T. F.: Effects of NOx and SO2 on the secondary organic aerosol formation from photooxidation of α-pinene and limonene, Atmos. Chem. Phys., 18, 1611-1628, doi: 10.5194/acp-18-1611-2018, 2018.

Zare, A., Fahey, K. M., Sarwar, G., Cohen, R. C., and Pye, H. O. T.: Vapor-Pressure Pathways Initiate but Hydrolysis Products Dominate the Aerosol Estimated from Organic Nitrates, ACS Earth Space Chem., 3, 1426-1437, 10.1021/acsearthspacechem.9b00067, 2019.

Tables

Table 1: Overview of α-pinene and β-pinene experiments

Experiment Description	**$[VOC]_0$[a] [ppb]**	**$[NO_X]_0$[a] & ($[NO_X]_{SS}$[b]) [ppb]**	**$[O_3]_{SS}$[b] [ppb]**	**$[OH]_{SS}$[b] [10^7 cm^{-3}]**
1. Gas-phase yield of ON and gas-phase $OrgNO_3$ (Section 3.1)	β-pinene 39→0 m-xylene 3.7	50 (20→30)	19→30	2.3±20%
2. Formation of HOM-ON (Section 3.3)	α-pinene 16.5	0.3 / 7.5 / 15.3[c] / 26.7 / 39.7 / 45.5 (0.3 / 1.8 / 3.7[c] / 5.7 / 8.7 / 10.4) / 52.9 / 59.1 / 83.3 / 137.8 (/ 12.4 / 15.8 / 26.8 / 72.2)	62 -152	4.5 -7.5
	β-pinene 37	3.9 / 53.8 / 113.6 / 194 (1.2 / 16.5 / 37.0 / 77.)	Not determined	Not determined
3. Effective uptake coefficients[d] (Section 3.4)	α-pinene 12.5	0.3 (0.3)	29	9.2±20%
	β-pinene 37	30 (4)	49	8.8±20%
4. $OrgNO_3$ in SOA (Section 3.5)	α-pinene 46	0.3 / 32.0 / 51.0 / 60.0 (0.3 / 10.4 / 17.5 / 19.5)	37 - 62	4.7- 7.7
	β-pinene 38	0.3 / 6.7 / 13.4 / 32.9 / 54.8 / 103 (0.3 / 5.1 / 9.5 / 21.7 / 35.5 / 45.7)	44 – 53	0.9 - 3.7

[a] subscript $_0$ refers to mixing ratio in the inflow
[b] subscript $_{SS}$ refers to mixing ratio in steady state
[c] average of two experiments at $[NO_X]_0$ of 15 and 15.5 ppb ($[NO_X]_{SS}$ of 3.6 and 3.75 ppb)
[d] in presence of ammonium sulfate seed aerosols

Figures

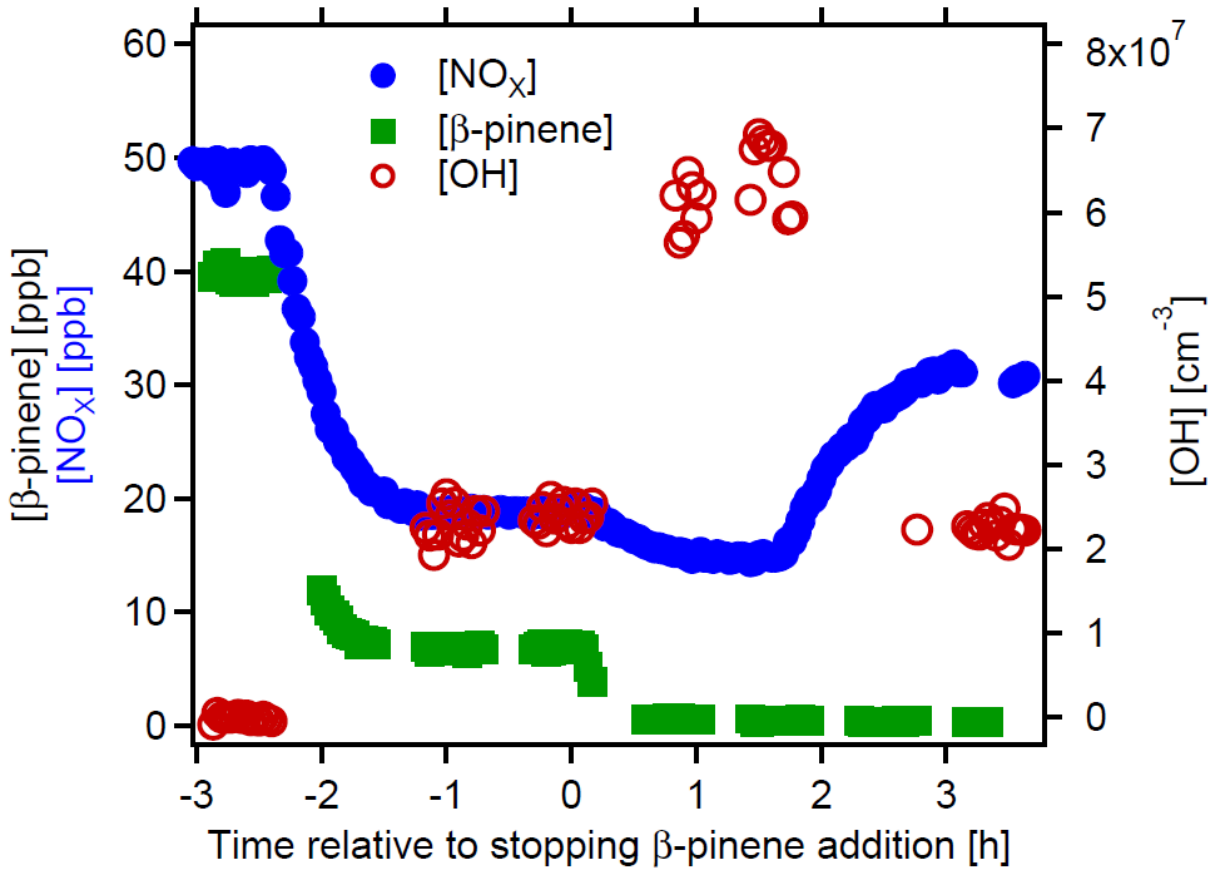

Figure 1: Time series of [β-pinene] (green squares, left scale), [NO_X] (blue circles, left scale) and [OH] (open brown circles, right scale). The experiment served to estimate the sum of organic nitrates (ON) formed in a mix of NO_X and β-pinene. M-xylene ([m-xylene]$_0$ ~ 3.7 ppb) was added to the chamber as tracer for OH. At time t = -2.4 h OH formation was induced by O_3 photolysis. At time t = 0 h, β-pinene addition was stopped and at time t = 1.7 h J(O^1D) was reduced to obtain the same [OH] as in presence of β-pinene at time -1 h.

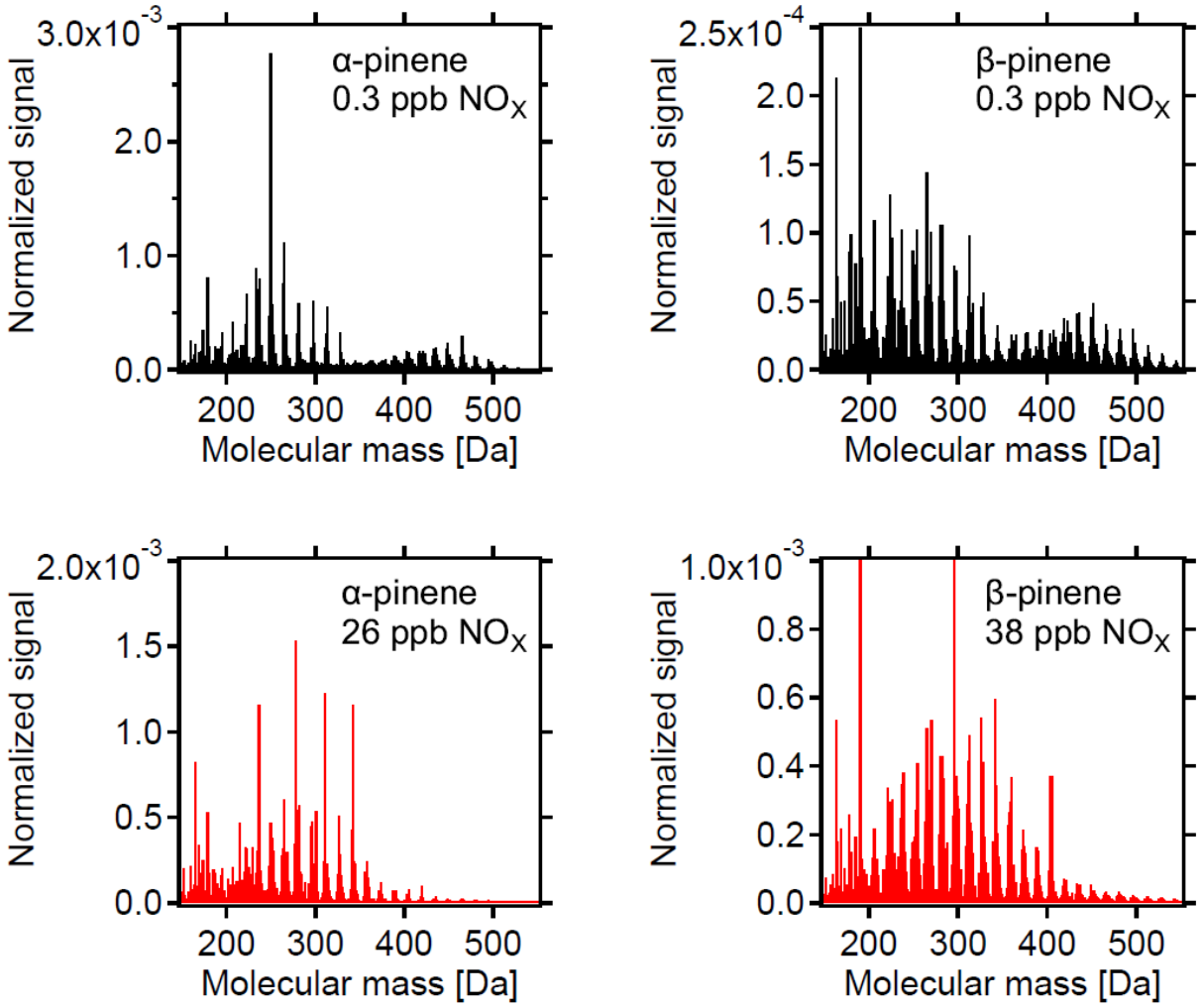

Figure 2. HOM spectra from photo-oxidation of α-pinene (left panels) and β-pinene (right panels) without NO_X addition (upper panels) and with NO_X addition (lower panels). NO_X concentrations in the α-pinene and β-pinene experiment were 26 ppb and 38 ppb, respectively. Background NO_X was 0.3ppb. The signals were normalized to the sum over all detected ions. For the α-pinene example, in the low NO_X case HOM monomers contribute ≈0.4 µg m^{-3} and HOM-ACC ≈0.3 µg/m^{-3}, whereas at 26 ppb NO_X HOM monomers contribute ≈0.4 µg m^{-3} and HOM-ACC less than 0.1 µg/m^{-3} (compare Figure 3).

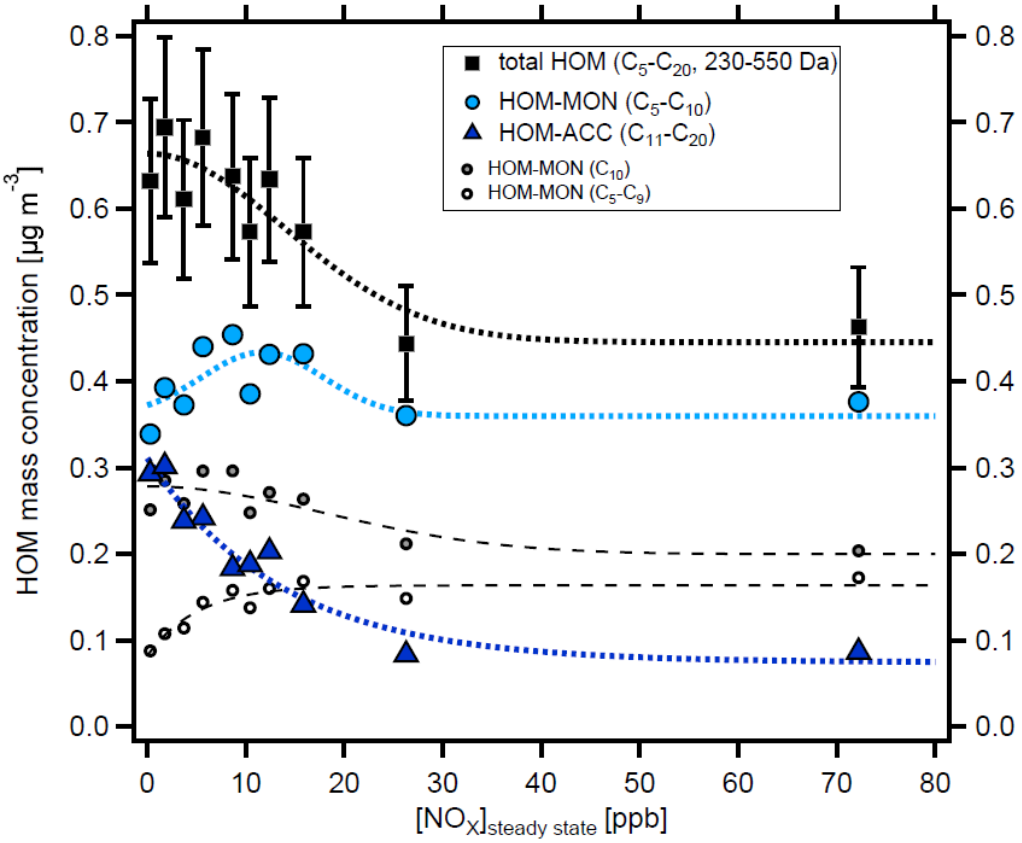

Figure 3. Mass concentration of HOM products in dependence on $[NO_X]_{SS}$ in α-pinene photo-oxidation experiments. C_5-C_{20} compounds with molecular masses 230-550 Da were added up for total HOM (black squares) and divided into HOM monomers (light blue circles) and HOM accretion products (blue triangles). The analysis is based on the assigned peaks (>90% of the total signal) and the sensitivity of 3.7×10^{10} molecules cm^{-3} nc^{-1} (suppl. section 1.2). HOM accretion products decrease with increasing $[NO_X]_{SS}$: at the lowest and highest NO_X levels of 0.3 ppb and 72 ppb HOM-ACC contribute 0.3 µg m^{-3} and 0.09 µg m^{-3}, respectively, to total HOM, whereas HOM monomers contribute about 0.4 µg m^{-3} over the whole range. More than 70% of HOM-ACC were suppressed at the highest $[NO_X]$ while HOM monomers remained about constant. The increasing importance of alkoxy radicals with increasing $[NO_X]_{SS}$ is indicated by the small circles: $C_{5\text{-}9}$ compounds (small open circles) arise in large parts from fragmentation of alkoxy radicals. They double from ≈0.9 to ≈1.8 µg m^{-3} at the highest $[NO_X]_{SS}$, whereas the C_{10} compounds (grey circles) drop by only about 30%. $C_{5\text{-}9}$ compounds must carry at least 7 O-atoms because the lower end of the mass range is set to 230 Da which is the molecular mass of $C_{10}H_{14}O_6$. Assuming that compounds in the selected mass range will contribute to SOA formation, the lower SOA yields at high $[NO_X]$ was due to the suppression of accretion products and increasing fragmentation via the alkoxy path played a minor role. Dashed and dotted lines save to guide the eye and have no further meaning. Concentrations were corrected as described in supplement section S1.2. Turnover ranged from 8.7×10^7 $cm^{-3}s^{-1}$ and 1.04×10^8 $cm^{-3}s^{-1}$ leading to correction factors in a range of 1.1 - 0.8. The correction factors were close to one thus did not add much uncertainty. Observed particle surface ranged from ~10^{-6} m^2m^{-3} to 6×10^{-5} m^2 m^{-3} resulting in correction factors between 1.0 and 1.45 with the highest correction factors at lower $[NO_X]_{SS}$ where new particle formation could not be suppressed.

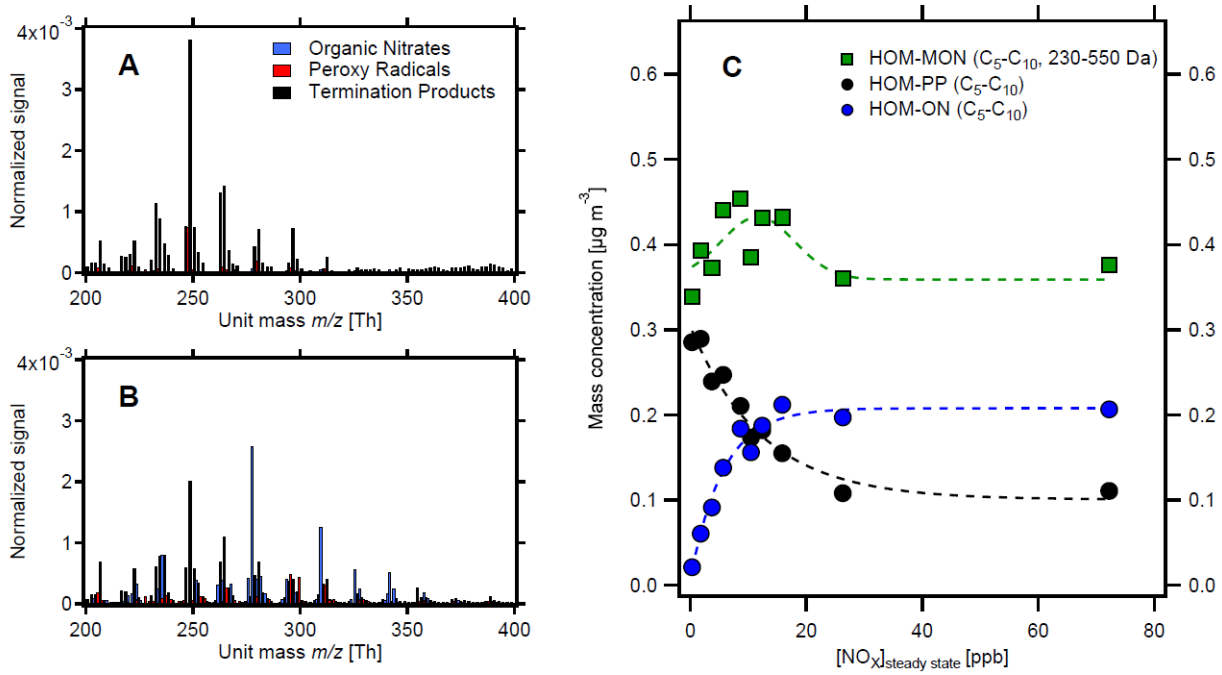

Figure 4: HOM pattern from α-pinene photo-oxidation at two NO_X levels in the monomer range. Panel A: low NO_X conditions ($[\alpha\text{-pinene}]_{SS}$ = 1.7 ppb, $[NOX]_{SS}$ = 0.3 ppb), Panel B: high NO_X conditions ($[\alpha\text{-pinene}]_{SS}$ = 1.0 ppb, $[NOX]_{SS}$ = 8.7 ppb). Black bars: HOM-PP termination products of reactions R3 and R4a. Blue bars: HOM-ON (organic nitrates). Red bars = HOM-RO_2 (peroxy radicals). The signals were normalized to the sum over all detected ions. Panel C: Mass concentrations of HOM monomers (green) in the molecular mass range 230-550 Da. HOM-ON (blue) are increasing with increasing $[NO_X]_{SS}$, HOM-PP (black) are decreasing, while the sum of all HOM-monomers remains about the same. At about 10 ppb $[NO_X]_{SS}$ HOM-ON make up half of the HOM monomers and at 26 ppb $[NO_X]_{SS}$ they make up about 50% of the total HOM (shown in Figure 3).

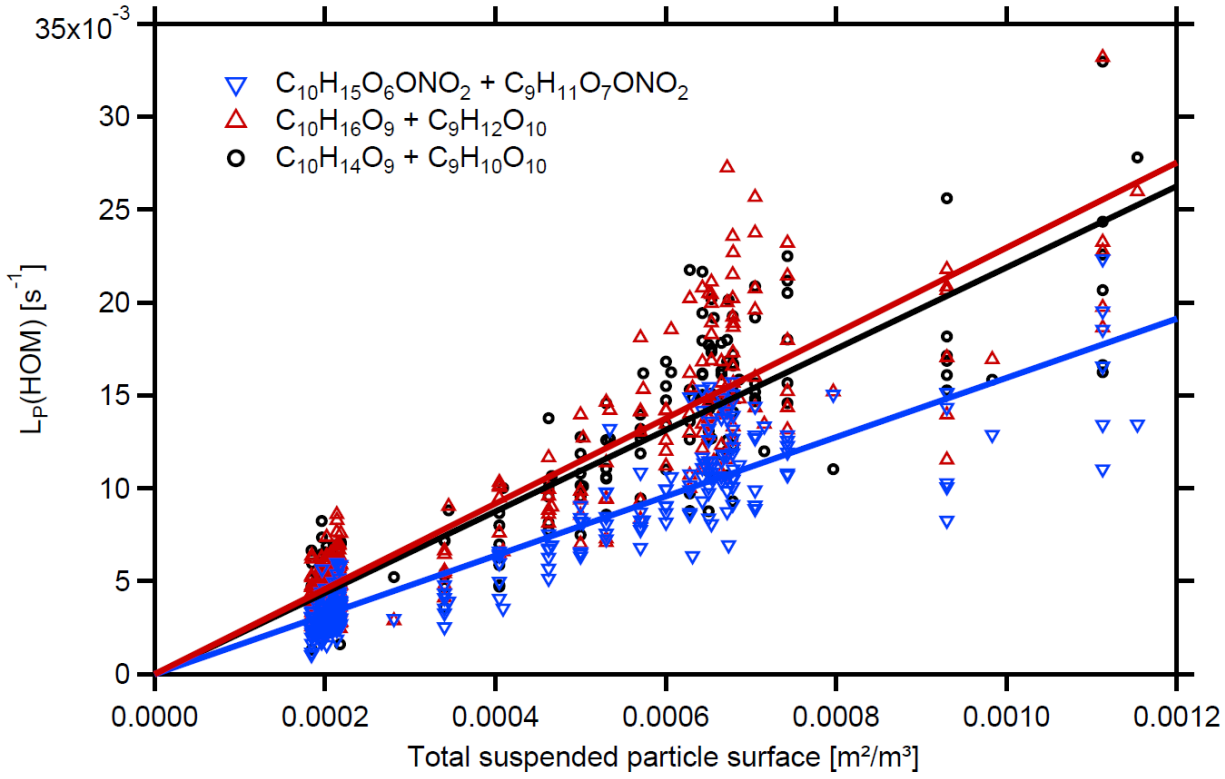

Figure 5: Plot of L_P(HOM) calculated by Eq.(6) versus particle surface area, S_P, for the examples of HOM-ON with a molecular mass of = 293 Da ($C_{10}H_{15}O_6ONO_2$ & $C_9H_{11}O_7ONO_2$), HOM-PP with a molecular mass of 280 Da ($C_{10}H_{16}O_9$ and $C_9H_{12}O_{10}$), and HOM-PP with molecular mass of 278 ($C_{10}H_{14}O_9$ and $C_9H_{10}O_{10}$). HOM from β-pinene photo-oxidation ($[\beta\text{-pinene}]_{SS}$ ~ 10 ppb, $[NOx]_{SS}$ ~ 4 ppb). Dividing the slopes by the respective $\bar{\nu}/4$ led to $f_{FS}\times\gamma_{eff}$ ~ 0.5 for the example HOM-ON and ~ 0.6 in the latter cases. The main uncertainty arises from the scatter of L_P(HOM) individual unit mass resolution data. Statistical errors of $f_{FS}\times\gamma_{eff}$ were about ± 5%.

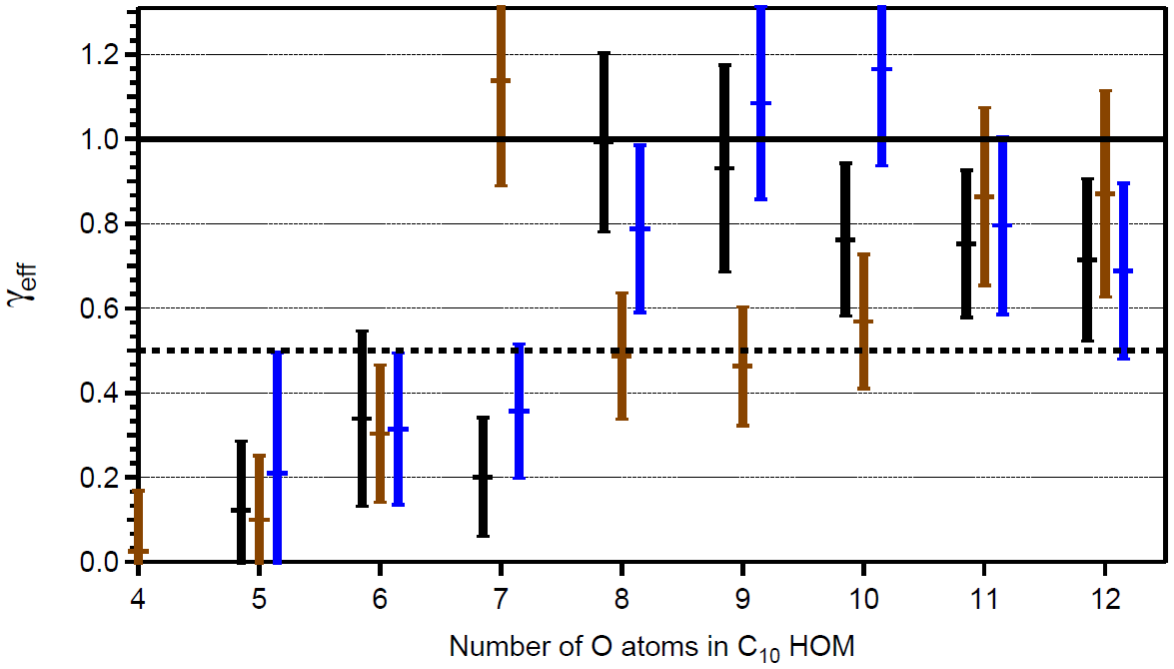

Figure 6: Effective uptake coefficients γ_{eff} for HOM-PP ($C_{10}H_{14}O_X$ black bars, $C_{10}H_{16}O_X$, brown bars) and HOM-ON ($C_{10}H_{15}O_XNO_2$, blue bars) in dependence of the number of O atoms in the respective HOM. HOM with different numbers of C, H, and O atoms, e.g. $C_{10}H_yO_x$ and $C_9H_{y-4}O_{x+1}$ HOM-PP, are treated together and the number of O-atoms is given for the C_{10}-HOM-PP. The second component, C_9-HOM-PP, has one O atom more. Data were taken from β-pinene photo-oxidation experiment with $[\beta\text{-pinene}]_{SS}$ ~10 ppb, $[NO_X]_{SS}$ ~ 4 ppb. The signal intensity for the $C_{10}H_{14}O_4$ and HOM-ON with 4 O-atoms was too low to allow reliable determination of γ_{eff} and the respective data is left out. Uncertainties in γ_{eff} arise from the determination procedure as shown in Figure 5. The black line indicates γ_{eff} = 1 and 0.5. An average Fuchs-Sutugin correction factor of 0.70 (d_p =175nm) was applied to calculate γ_{eff}.

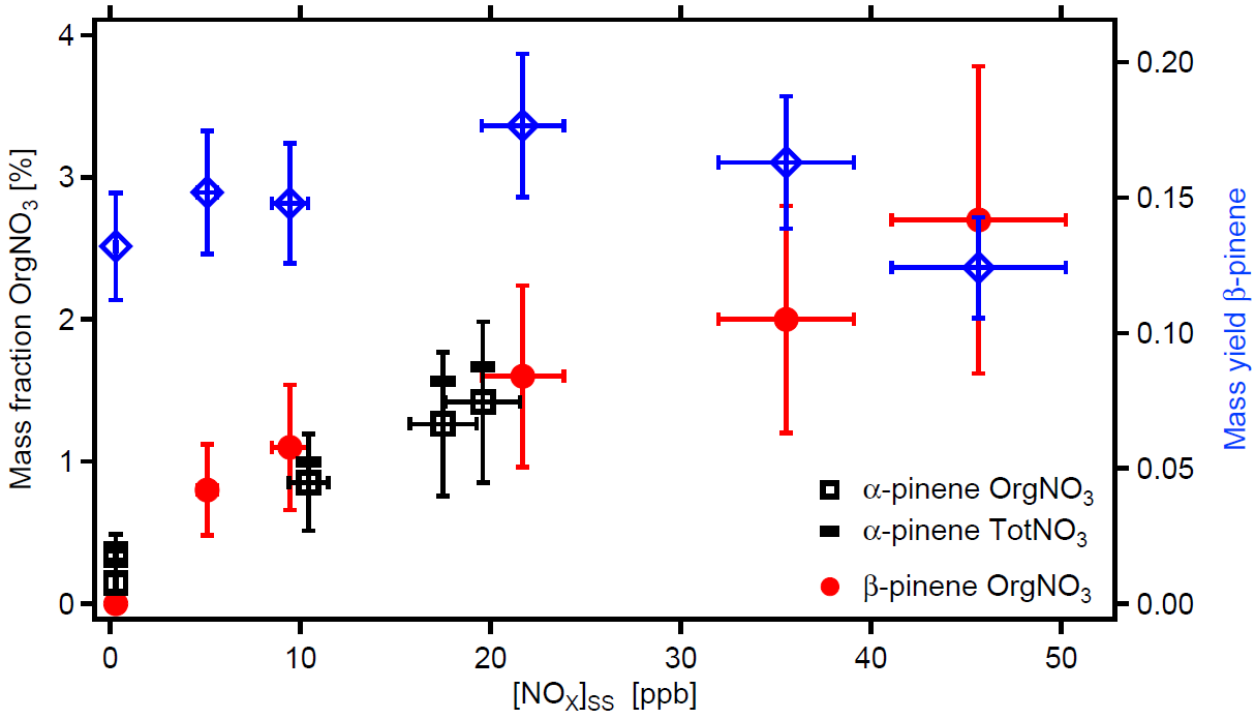

Figure 7: Mass fraction of organic bound nitrate ($OrgNO_3$) in SOA in dependence of $[NO_X]_{SS}$ (left y-axis). Black squares and red circles show data measured from α-pinene and β-pinene, respectively. SOA mass yields during the respective experiment are shown at the example of β-pinene (blue diamonds). The SOA load ranged from 11 µg m^{-3} to 23 µg m^{-3} with an average of 16±5 µg m^{-3}. The data are corrected for wall losses of HOM. In absence of OH, $[\alpha\text{-pinene}]_0$ was around 46 ppb, $[\beta\text{-pinene}]_0$ was around 37 ppb. NO_X was added at different amounts with $[NO_X]_0$ up to 103 ppb. Due to losses in reactions with OH and formation of organic nitrates, $[NO_X]$ decreased to the $[NO_X]_{SS}$ levels shown here. Uncertainties in NO_X data are estimated to ± 10%, uncertainties in SOA masses to ± 10 %, and uncertainties in the content of $OrgNO_3$ are estimated to ± 40%. The black bars indicate the fraction of total nitrate ($TotNO_3$, left scale) for the example of α-pinene, which is dominated by organic nitrate.

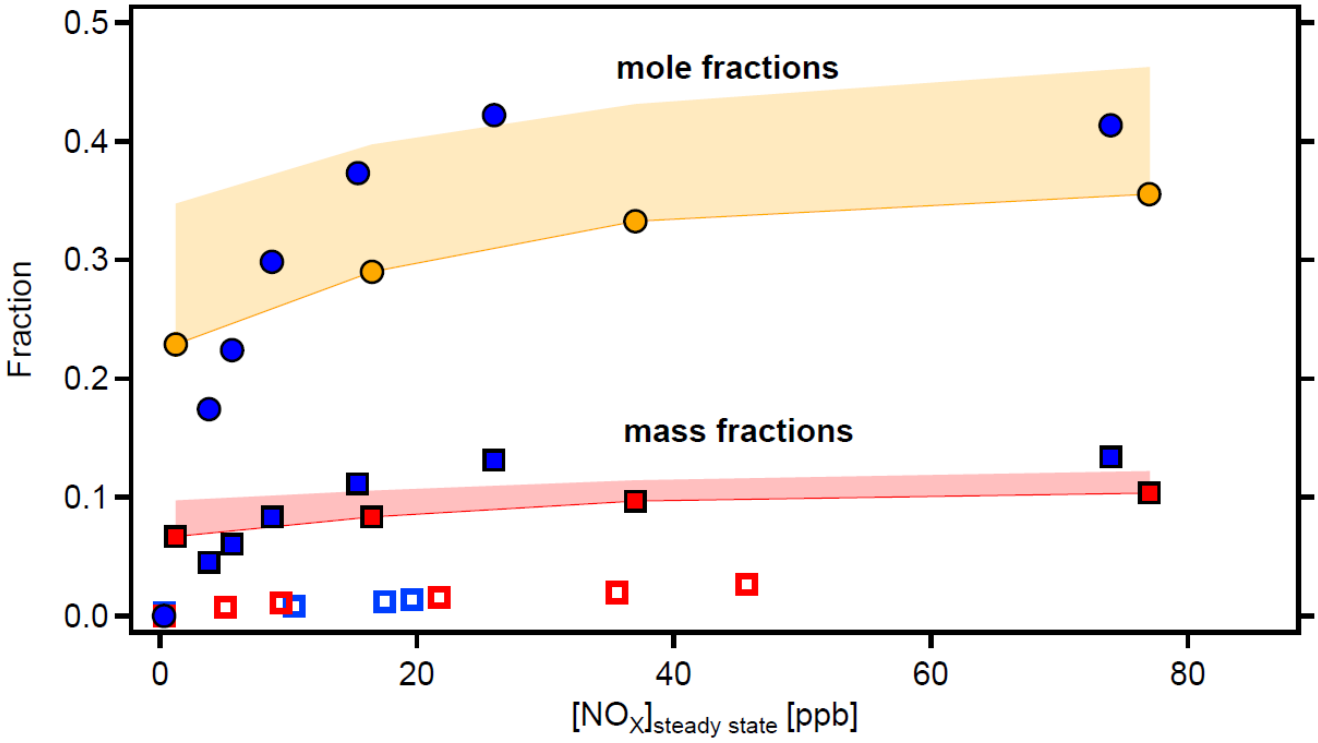

Figure 8: Molecular fractions of organic bound nitrate ($OrgNO_3$, filled circles) and mass fractions of $OrgNO_3$ (squares) as a function of $[NO_X]_{SS}$. Data from α-pinene (blue symbols) and β-pinene (orange and red symbols and areas). *Molecular fraction* of $OrgNO_3$ and HOM-ON are the same by definition. The mass fraction of $OrgNO_3$ in the gas-phase HOM is significantly higher than in the particulate phase as determined by AMS (open blue and red squares).
The areas in orange and red give the potential error for β-pinene due to unresolved progressions and overlap of organic nitrates with peroxy radicals (as explained in text).

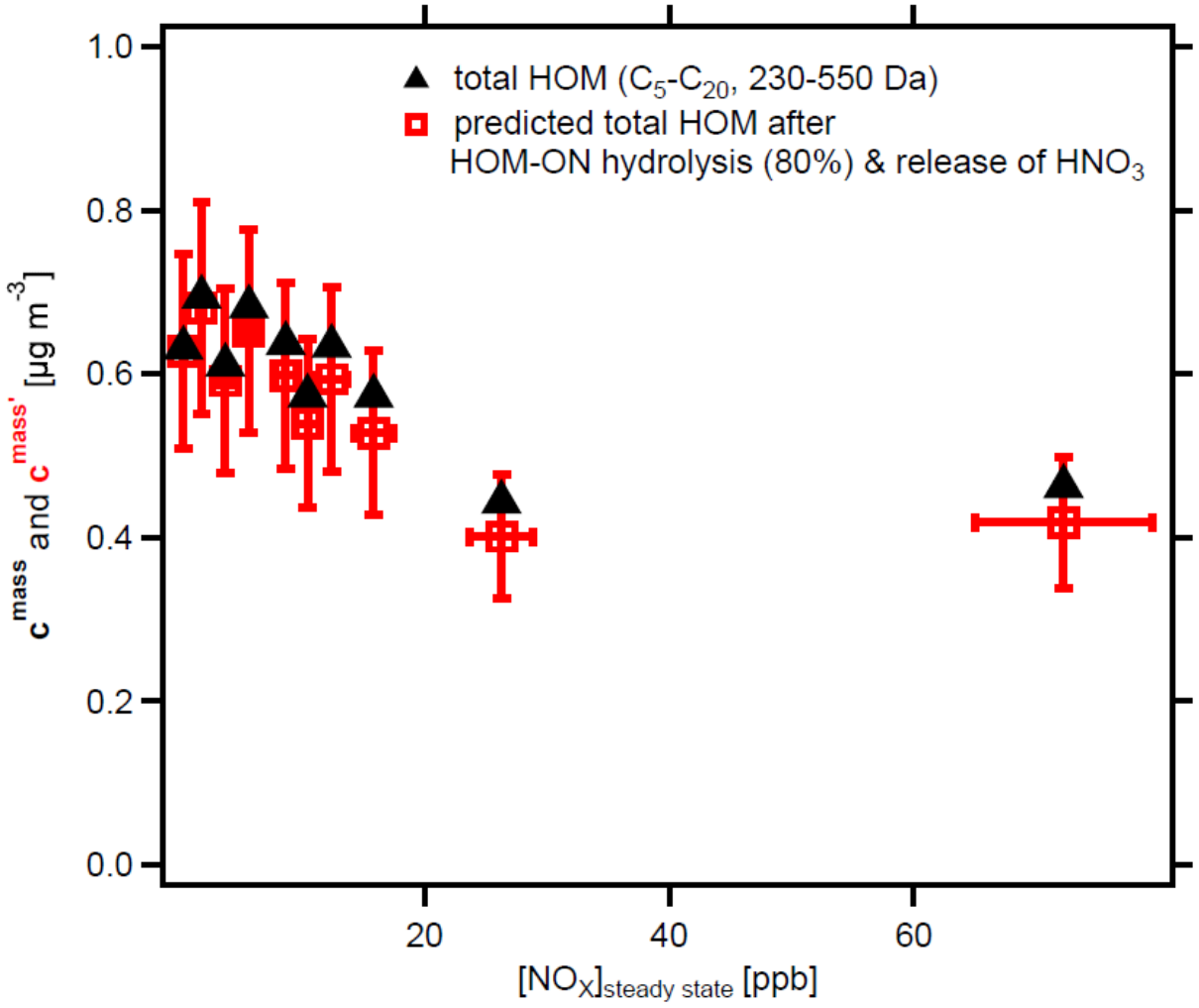

Figure 9. Mass concentrations of total HOM (C_5-C_{20}) with molar masses between 230 to 550 Da. Black triangles show mass concentrations c^{mass} as determined. Red squares show $c^{mass'}$ i.e. the resulting SOA mass after considering $OrgNO_3$ loss by hydrolysis and evaporation of HNO_3. $[\alpha\text{-pinene}]_{SS}$ = 0.9 to 2.2 ppb, $[NO_X]_0$ up to 125 ppb, $[NO_X]_{SS}$ = 0.3 to 74 ppb. The effect of hydrolysis of 80% of the organic bound nitrate has no substantial effect on the SOA mass. Analysis is based on assigned molecular formulas (>90% of the total signal) applying the sensitivity of 3.7×10^{10} molecules cm^{-3} nc^{-1} (supplement section 1.2).